The International Journal of Advanced Manufacturing Technology
https://doi.org/10.1007/s00170-020-06069-0

ORIGINAL ARTICLE

Cooling of motor spindles—a review

Berend Denkena [1] · Benjamin Bergmann [1] · Heinrich Klemme [1]

Received: 15 June 2020 / Accepted: 7 September 2020

Abstract
Thermally induced loads in motor spindles can cause a number of undesired effects. As a result, the process capability of spindles, and thus, the productivity of a process can decrease. Future motor spindles will be exposed to higher mechanical and especially thermal loads due to trends aiming to increase power densities and maximum speeds. These trends are amplified by increasingly powerful drive concepts and developments in bearing technology. Therefore, researchers assume that it will not be possible to raise the performance potential of spindles due to insufficient cooling of its heat sources. A series of different cooling concepts have been researched and developed in recent decades. These developments have been made for different purposes. They also differ considerably in terms of their cooling principles and cooling performance. In this article, these cooling approaches and the motivations for their development are described. Firstly, the causes of heat development in motor spindles are described in a historical context. Subsequently, the effects of heat development on the manufacturing-relevant properties of motor spindles are revealed. Finally, current deficits in the area of spindle cooling and the need for the development and transfer into industrial practice of more efficient and cost-effective cooling concepts to overcome future challenges are discussed.

Keywords Motor spindle · Cooling · Spindle design · Manufacturing accuracy · Heat pipes

1 Introduction

The achievable accuracy of machine tools has been continuously increasing over the last decades. In Taniguchi [1], the development of the manufacturing possibilities with regard to achievable machining accuracy since the 1940s (Fig. 1) is shown. Future developments in research and industry will lead to further increases in manufacturing accuracy of machine tools. This development is driven by increasing demands for accuracy of workpieces. Thus, achievable accuracy is also a crucial sales argument for machine manufacturers.

The achievable manufacturing accuracy is significantly influenced by the thermal and mechanical properties of spindle main drives and their rotational accuracy [2–6]. A spindle drive is a drive that generates the rotary cutting motion to cut materials. The cutting motion can be carried out by rotating the workpiece (e.g., lathes) or the tool (e.g., drilling or milling machines). All spindles are designed as shaft-bearing-systems. A rotary shaft is coupled to a surrounding spindle housing by at least one bearing [7]. Spindle drives have two basic main functions [8]. They ensure the rotation of the workpiece or tool in space. Moreover, they transmit the necessary energy for the cutting process. Due to the comparatively low purchase and operating costs, roller bearing spindle systems are mainly used in current manufacturing practice [9]. The majority of these spindles have an integrated motor drive [8]. Such spindles are called motor spindles. As a result of the conversion of electrical energy into mechanical energy, electrical losses in the form of heat occur. Friction between the bearing elements causes additional heat, which acts as a load on the spindle system. Increasing relative speeds between rotating components and the surrounding fluid (usually air) leads to the increase in heat caused by fluid friction [10]. For these reasons, a motor spindle represents the main heat source in machine tools [11]. The proportion of losses occurring in motor spindles is shown in Fig. 2 exemplarily for an IM grinding spindle at a maximum speed of 36,000 min^{-1} and maximum power of 7 kW.

✉ Heinrich Klemme
klemme@ifw.uni-hannover.de

Berend Denkena
denkena@ifw.uni-hannover.de

Benjamin Bergmann
bergmann@ifw.uni-hannover.de

[1] Institute of Production Engineering and Machine Tools (IFW), Gottfried Wilhelm Leibniz Universität Hannover, An der Universität 2, 30823 Garbsen, Germany

Published online: 21 September 2020

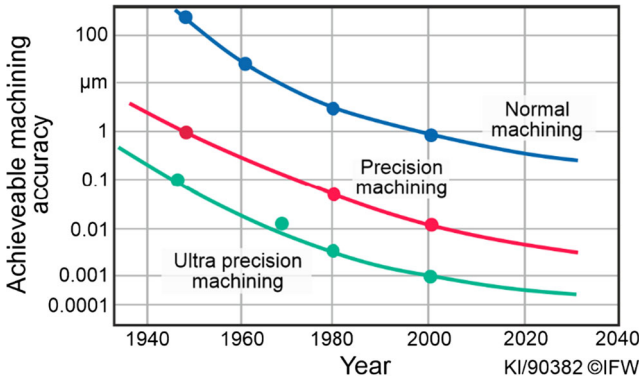

Fig. 1 Evolution of the achievable machine accuracy according to [1]

Heat generation causes a number of undesirable effects. These effects can ultimately lead to machining inaccuracies or even to machine failures. To counteract these effects, spindle cooling concepts have been researched and developed in recent decades. The cooling of heat sources is the most common and effective way to reduce or avoid undesirable effects [12]. However, the requirements for cooling concepts are changing as a result of emerging trends in the field of motor spindle development such as increasing spindle power and power densities.

To outline future requirements for spindle cooling concepts from a historical context, Section 2 of this article deals with the development of motor spindles for machine tools in recent decades. Section 3 deals with heat-related effects that limit the performance of motor spindles. Section 4 provides an overview of concepts for cooling motor spindle components. The cooling concepts are evaluated in terms of their technical, economic, and ecological properties. The aim of this article is to identify deficits between the current situation and present future challenges in the development of motor spindle cooling systems (Section 5).

2 Development of motor spindles

Until the 1980s, gear spindles were used to achieve high speeds [8]. This drive concept was still state of the art in the early 1990s [13]. At that time, very high spindle speeds could only be achieved by using magnetic bearings. However, this expensive and complex technology did not find its way into industrial practice. Technological advances in the fields of bearing and lubrication technology as well as the development of more powerful and efficient drives beginning in the mid-1990s led to an increasing market relevance of motor spindles [8, 14]. At the beginning of the 1990s, rolling bearings with ceramic rolling elements (hybrid bearings) were not yet an alternative for conventional steel bearings [15] due to their cost and performance. However, this development was the key technology for increasing spindle speeds at the end of the 1990s [16]. The so-called specific speed parameter $n \cdot d_m$ is used as an indicator for evaluating the development of new rolling bearing technologies. This indicator is calculated by the product of the speed at the operating point speed n (in min^{-1}) and the mean bearing diameter d_m (in mm). The $n \cdot d_m$ parameter defines the maximum permissible speed for standard designs of a bearing type. In the early 1990s, the achievement of values between 1.0 and 2.0 × 10^6 mm/min was still revolutionary [14]. At the beginning of the 2000s, however, research was already being conducted to develop $n \cdot d_m$ values in the range of 3.5–4.0 × 10^6 mm/min [17, 18]. Since the beginning of the 2010s, bearings with $n \cdot d_m$ values of 4.0 × 10^6 mm/min and more have been offered by many rolling bearing manufacturers [19–22]. Improved converter technologies have also made it possible to reduce harmonious motor supply fractions and the resulting harmonic losses. This also led to a reduction of heat loss and an increase in power density of motor spindles [8]. Further development of permanently excited synchronous motors (PMM) allowed further increases in power density and smaller spindle sizes to be achieved with

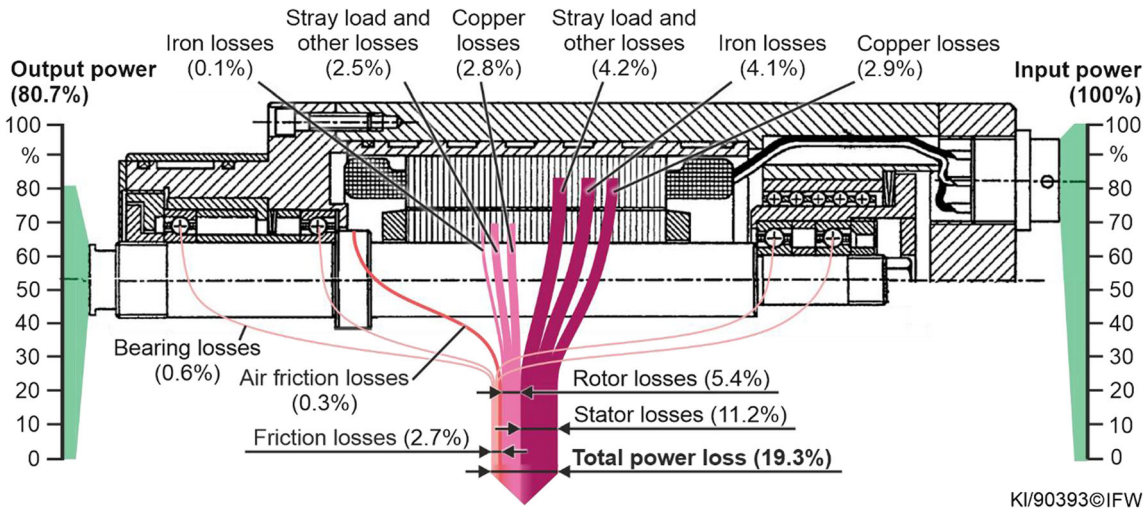

Fig. 2 Proportion of losses for an IM grinding spindle according to [10]

the same or even higher power than with induction motors (IM). Nevertheless, IM are still frequently used today in main spindles. The reasons are the lower acquisition costs due to the absence of permanent magnets (rare earths elements) in the rotor. Moreover, PMM are associated with demagnetization risks. Presently, motor spindles with rolling bearings have largely replaced spindles with alternative drive concepts such as gear-driven spindles, direct-drive spindles, and belt-driven spindles. Due to the low acquisition costs, belt-driven spindles are nowadays mainly used in the lower machine price segment at speeds of up to 15,000 min^{-1}, if there are no high demands for manufacturing accuracy [23]. Direct drive spindles are primarily used in auxiliary drives [24]. Gear spindles are still superior to motor spindles in terms of high torque ratings [25]. However, due to continuous further developments, the operating ranges of today's motor spindles could be extended to significantly larger speed, power, and torque ranges. Figure 3 illustrates the maximum speeds of commercially available motor spindles with the corresponding maximum power. This representation is based on [8] and was supplemented with data from market research carried out in 2019. For this purpose, the product catalogs of twelve leading motor spindle manufacturers were analyzed. Figure 3 depicts distinct trends towards higher motor outputs and higher maximum speeds. This trend is also confirmed in [26]. Increases in spindle speed and motor power lead to increasing metal removal rates and thus reduce machining time. Tools with larger diameters can be used to increase the material removal rate. The feed per tooth can also be increased by augmenting the spindle speed. By increasing the cutting speed, higher surface qualities can be achieved during finishing [15].

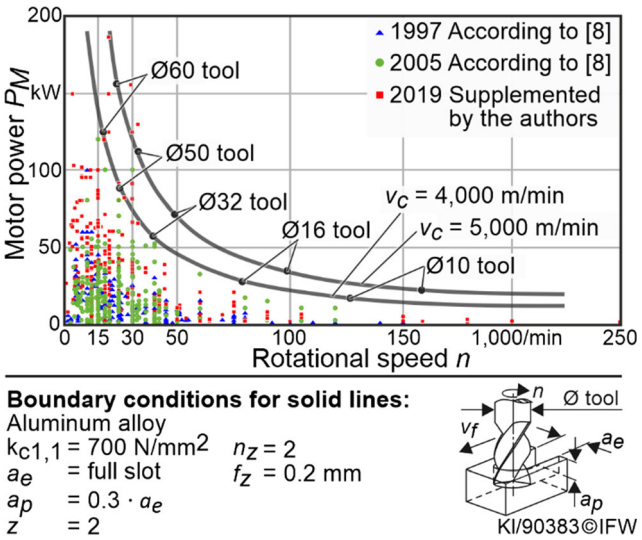

Fig. 3 Evolution of maximum speed and motor power according to [8]

Despite all innovations and performance enhancements of the recent decades, the shaft-bearing-system is still a bottleneck for new spindle developments [8]. Especially decreasing the shaft temperature is of central importance to improve the performance of motor spindles. The reasons for this are explained in the following section.

3 Heat in motor spindles

Heat losses can lead to the following effects [10, 27]:

- Geometry errors on the workpiece due to thermo-elastic deformation of the spindle,
- Process instability and consequently surface defects due to varying bearing preload,
- decrease of available electric motor power due to decreasing flux density,
- reduced motor lifetime due to faster aging of insulation materials,
- increase in non-productive times as a result of a longer period of time to reach a thermally steady state, and
- reduced bearing lifetime due to increasing tribological wear.

In Fig. 4, the thermal chain of these effects is demonstrated according to [28]. The thermo-mechanical properties of the

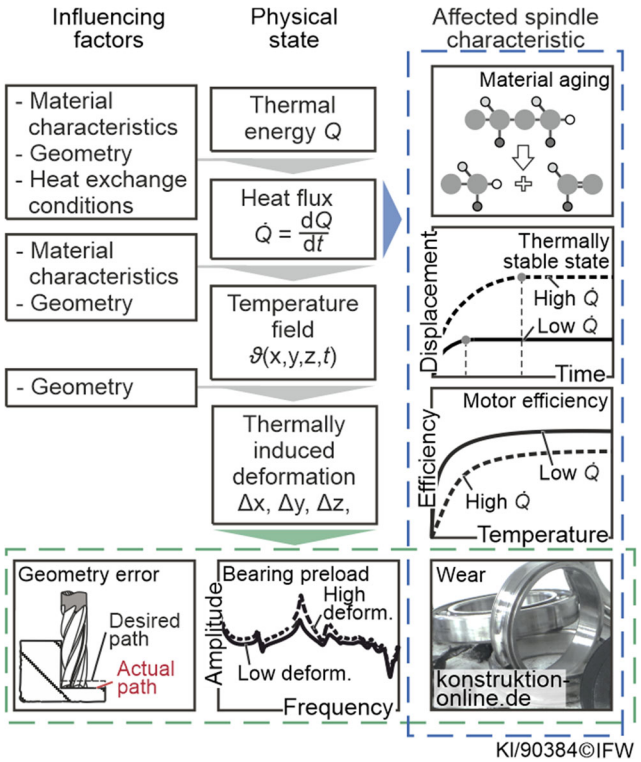

Fig. 4 Thermal effects within a motor spindle according to [28]. Supplemented by the authors

shaft-bearing-system significantly influence the accuracy of the relative motion between the tool and workpiece. Motor spindles are therefore the main sources of machining errors [10, 11]. However, a spindle system cannot be described by two isolated thermal and mechanical subsystems as interactions exist between these systems. These interactions are explained in the following subsections. Whether an insufficient machining result was obtained as a result of insufficient thermal or mechanical properties of the spindle cannot always be assumed. A separation between thermal, mechanical, and geometric errors of the machine tool, as described in [29], is therefore not permissible when considering a spindle system individually.

Challenges due to heat in motor spindles are currently being addressed by the industry and research. The efforts to improve the thermal properties of motor spindles with roller bearings can also be evaluated on the basis of articles published on this subject since 1990 (Fig. 5). All relevant articles on the subjects of "spindle cooling," "spindle temperature," and "spindle thermal" accessible at webofknowledge.com have been used for this evaluation. Since 2011, a significant increase in scientific articles is noticeable. Compared with 2010, the number of articles published annually has increased more than fourfold to the present time.

3.1 Influence of thermal load on manufacturing accuracy

Deviations between the nominal and the actual position of the TCP can lead to manufactured dimensions being beyond the tolerances to be maintained. In a best case scenario, the workpiece can be reworked. This is to be associated with considerable additional time and effort. In the worst case, the workpiece must be rejected [30]. During manufacturing, a variety of factors can lead to these deviations. These include machine errors (e.g., geometry and position errors), process errors (e.g., tool displacement and vibrations), and errors due to inadequate properties of auxiliary equipment. In order to evaluate the relative relevance of each source of error on the resulting total error, error budget analyses can be used [31]. The error budgeting method can link error sources to target values via coupling mechanisms [31–33]. For this purpose, a multi-physical model of the relevant machine behavior is established. Subsequently, the influences of individual parameter value changes on the TCP displacement are determined. The determined influences are indicated as sensitivities [33] or uncertainties [31]. A result of such an error budgeting is illustrated in Fig. 6 for analyses of a 3-axis conventional high-speed machining center and a 3-axis ultra-precision micro milling center. Accordingly, the share of thermally induced expectable error E_M in the overall machining error is 7% (ultra-precision micro milling center) and 17% (high-speed machining center), respectively. Besides tool deflection, the thermally induced error thus has the second largest influence on the total uncertainty error in the case of high-speed machining.

The influence of temperature on manufacturing precision cannot be quantified universally. Figure 6 is therefore only to be understood exemplarily. The displacement depends too much on the respective machine structure, kinematics, and other mechanical and thermal boundary conditions. However, it is well known that thermally induced errors account for a considerable proportion of the total manufacturing error of workpieces [33, 34]. It is estimated that thermal machine tool error due to Tool Center Point (TCP) displacement accounts for up to 50% of workpiece rejects [29]. These apparent contradictions with regard to the influence of heat result on the one hand from the fact that the studies from [29, 31] are not directly comparable. In addition, numerous measures are applied in manufacturing practice to minimize the abovementioned influences. Errors such as tool displacement or trajectory errors can often be predicted deterministically or are reproducible. Consequently, measures to reduce these influences are more effective. On the other hand, thermal errors are not only caused by internal heat sources or heat sinks, but also by varying ambient conditions. These include room layer temperatures, solar radiation, heat from auxiliary equipment,

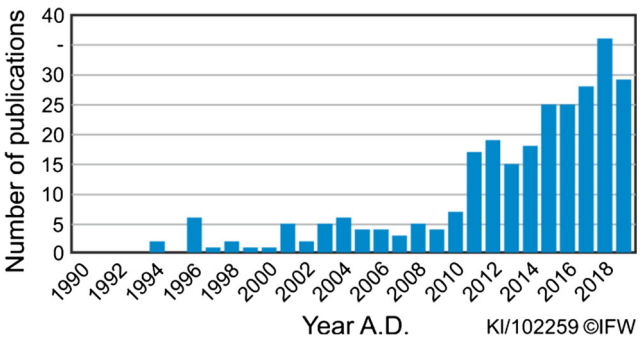

Fig. 5 Development of publications on spindle cooling from 1990–2019

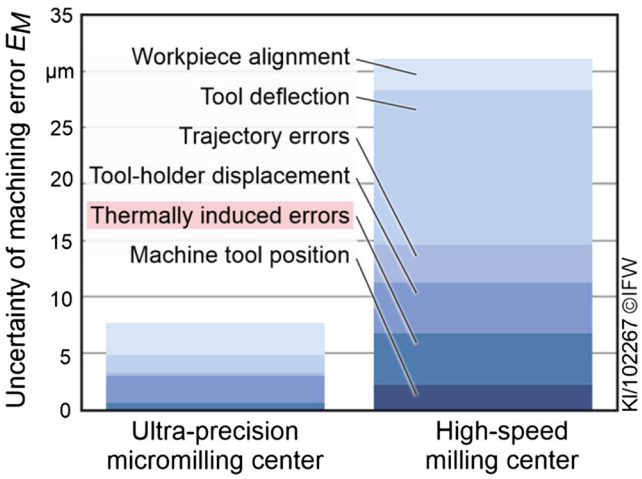

Fig. 6 Error budgets of an ultra-precision and a conventional machining center according to [31]

and other influences. These variables are often difficult or impossible to quantify and therefore cannot be taken into account for countermeasures.

However, there is no work known from the current state of knowledge whose results allow generally valid statements to be made about the sole proportion of spindle elongation in thermally induced manufacturing defects. In practice, TCP displacements due to spindle elongation amount to values in the one to two-digit micrometer range. Even displacements of up to several tenths of a millimeter can occur [35]. Research in which the influence of temperature rise on the spindle elongation is quantified can be found, for example, in [11, 36–43]. In general, the displacement of the TCP can be described by the superposition of the thermally induced displacements of the machine components within the thermo-mechanical effect chain. Figure 7 shows an example of the thermo-elastic expansion Δz of two joined bodies with lengths l_1 and l_2 and coefficients of thermal expansion γ_1 and γ_2. The expansion can be described by the linear correlation according to Eq. 1. The values $\theta_{1,1}$ ($\theta_{1,2}$) and θ_0 represent the mean temperatures of the bodies in warm and initial states.

$$\Delta r = \gamma_1 \cdot \int_0^{l_1} \left(\theta_{1,1} - \theta_0\right) dz + \gamma_2 \cdot \int_{l_1}^{l_2} \left(\theta_{1,2} - \theta_0\right) dz \quad (1)$$

In practice, the influence of the spindle position can be minimized by two approaches. One approach is compensation, which also includes the cooling techniques discussed in this paper. The application of special materials (e.g., [44, 45]) and targeted heating (e.g., [46, 47]) as well as design adaptions (e.g., [48, 49]) are also assigned to compensatory measures. Another approach is the application of corrective measures. Here, the thermo-elastic displacements are determined by means of models or measurements. Subsequently, a correction matrix is added to the target value matrix of the control system [50]. Such corrective measures are often carried out for thermal stabilization of the entire machine or individual structural units (e.g., [51–60]). However, as motor spindles are usually the main sources of heat, there are a series of studies that deal with the modeling of spindles and their metrological investigation for the identification of correction values (e.g., [41, 61–72]). A review on this topic is given in [73]. A major disadvantage of correction measures is the often time-consuming development of sufficiently accurate models and associated extensive experiments. Moreover, particularly critical are varying displacements, which can occur during machining due to varying operating conditions. Such time-dependent changes are often not considered by less complex correction models. Due to the high relevance of thermally induced displacement, however, correction approaches are applied in industrial practice [31] to minimize the most significant share of error.

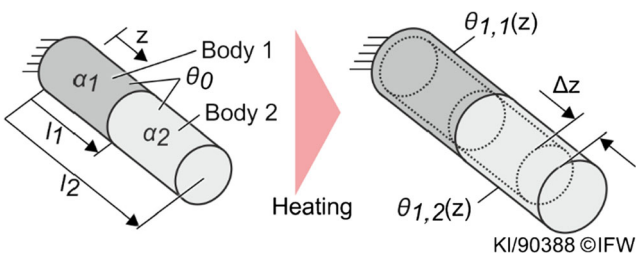

Fig. 7 Thermo-elastic deformation of two coupled solid bodies

In addition to these macroscopical geometrical errors due to TCP displacement, thermo-elastic deformation of the shaft-bearing system can also indirectly influence the surface quality of a workpiece. The reason for this is the variation of the dynamic properties due to a thermo-elastically induced variation of the contact conditions between rolling elements and bearing rings described in Section 3.2. In [74], Fujii et al. refer to the contradiction between increasing preload and the associated tribological temperature increase in the bearings. The authors note a significant temperature increase in the bearing inner and outer rings due to the increase in bearing preload. Fujii et al. determined the arithmetic average roughness Ra of the component surfaces for two different spindle speeds by varying the bearing preload in three steps. The resulting surface qualities for a spindle speed of 7,800 min^{-1} are shown for three preload values in Fig. 8. Thermally induced increase in bearing preload from 550 to 2,080 N leads to a decrease of Ra by about 50%. Although a large preload leads to a decreasing surface roughness, in this paper as well as in [75], it has been observed that an excessive preload is not appropriate for achieving high machining accuracy. High preloads lead to increasing tribological effects and thus to reduced bearing lifetime.

3.2 Influence of heat on bearing properties

Bearing friction losses which occur during spindle operation increase exponentially with rotational speed [10, 15]. As a result, at high speeds the friction converted into heat can amount to several hundred watts [76]. The heat can generally

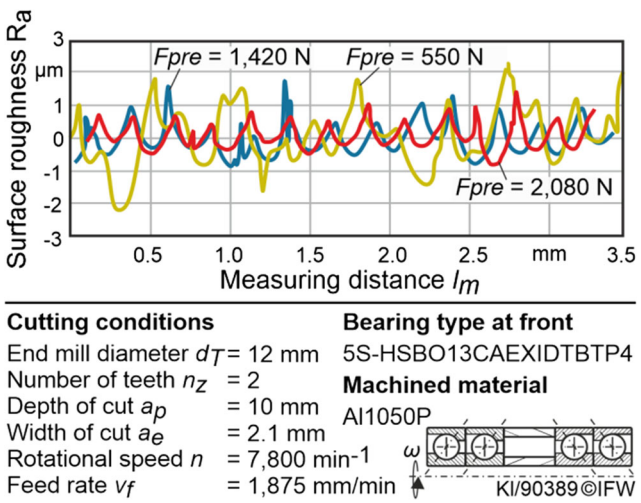

Fig. 8 Effect of bearing preload on workpiece surface quality (reworked from [74])

be dissipated less effectively from the inner rings than is the case of the outer rings. This is due to the better thermal coupling of the outer bearing rings to the housing [50]. As a result, the inner rings expand thermo-elastically. In addition, bearing inner rings can be subjected to heat losses from the motor [77]. Moreover, gravitational, centrifugal, and process forces, the lubricant and the applied coolant strategy, the obligatory sealing air, and environmental influences affect the thermo-mechanical behavior of a spindle. These loads overlap and partly interact with each other. As a result of these loads, the contact conditions between rolling elements and bearing rings and consequently the mechanical properties of a spindle system change. The complexity of these interactions practically makes it impossible to analytically describe the thermo-mechanical behavior of shaft-bearing systems [77].

The mechanical properties of a shaft-bearing-system are significantly influenced by the combined bearing preload [78]. The combined preload consists of the initial preload, i.e., the preload that is set during spindle assembly, and the portion of the preload due to mechanical and thermal influences. The actual applied bearing preload can normally not be measured during operation. Instead, the bearing clearance e is used as a variable to characterize the bearing preload indirectly. The bearing clearance describes the distance by which one bearing ring can be moved from one limiting position to the other in radial (radial clearance e_{rad}) or axial direction (axial clearance e_{ax}) in relation to the respective other rings, without any force being measured (Fig. 9b).

However, a change of e_{ax} has only minor effects on the contact conditions between rolling elements and bearing raceways. The reason for this is the negligible influence of variation of e_{ax} on the bearing osculation κ [77]. The bearing osculation is the quotient of the rolling element radius r_e and the groove radii $r_{rw,i}$ or $r_{rw,o}$. For angular contact ball bearings, the bearing osculation is calculated according to Eq. 2.

$$\kappa = \frac{r_{re}}{r_{rw}} \cdot 100 \tag{2}$$

For this reason, the variation of e_{rad} is considered a measurand for the evaluation of the thermally induced influence on the bearing contact conditions [77]. The thermally induced variation of radial clearance Δe_{rad} is calculated according to [77] by Eq. 3.

$$\Delta e_{rad}(\vartheta_{b,i}, \vartheta_{b,o}) = 2 \cdot \left(r_{gr,o} \cdot \gamma_{m,o} \vartheta_{\cdot b,o} - r_{re} \cdot \gamma_{m,re} \cdot \left(\vartheta_{b,o} + \left(\frac{\vartheta_{b,i} - \vartheta_{b,o}}{2} \right) \right) - r_{gr,i} \cdot \gamma_{m,i} \cdot \vartheta_{b,i} \right) \tag{3}$$

Hereby, $r_{gr,o}$ and $r_{gr,i}$ are the distances between the bearing axle and the bearing groove at the outer and inner ring. The coefficients of thermal expansion of the bearing inner and outer ring material as well as of the rolling element material are given by $\gamma_{m,i}$, $\gamma_{m,o}$, and $\gamma_{m,re}$. The mean temperatures of the bearing outer and inner rings are given by $\theta_{b,o}$ and $\theta_{b,i}$.

A further characteristic parameter describing the contact conditions is the contact angle β. This parameter is related to e_{rad} by Eq. 4.

$$\cos(\beta_0) = 1 - \frac{e_{rad}}{2 \cdot (r_{gr,i} + r_{gr,a} - 2 \cdot r_{re})} \tag{4}$$

The initial manufacturing contact angle is given by β_0 (Fig. 9a). For angular contact ball bearings of 70-, 719-, and 72-series, it is usually 15°, 20°, or 25°. An arrangement of these bearings within an O-arrangement is the most common configuration in main spindles [50]. For an O-arrangement, the manufacturing contact angle β_0 shifts towards larger values as a result of the preload force F_{pre}, which is set during spindle assembly (Fig. 9c). During bearing operation, the contact angle varies as a result of external forces F_{ext}, centrifugal forces F_{ce}, gyroscopic torques M_{gt}, and thermal expansion of the bearing components (Fig. 9d). As a result of this load spectrum, two different operating contact angles occur at the inner bearing ring ($\beta_{op,i}$) and at the outer bearing ring ($\beta_{op,o}$).

According to Eq. 3, lower values of γ of the bearing components lead to an increase of e_{rad} and thus to higher permissible thermal load capacities of the bearings. In particular, the thermally induced expansion of the bearing rings constitutes a significant part of the reduction of e_{rad} [79]. Figure 10 illustrates the correlation between the temperature-induced variation of e_{rad} and the resulting increase of combined preload F_{com} according to [80] in terms of an O-arrangement with bearing type 7014. Even a slight increase in the temperature difference $d\theta_{in/out}$ by a few Kelvin leads to an increase in preload of several kilonewtons.

By increasing F_{pre} resulting from decreased e_{rad}, a tribologically induced reduction of bearing lifetime or even sudden bearing damage can occur (Fig. 11, red paths).

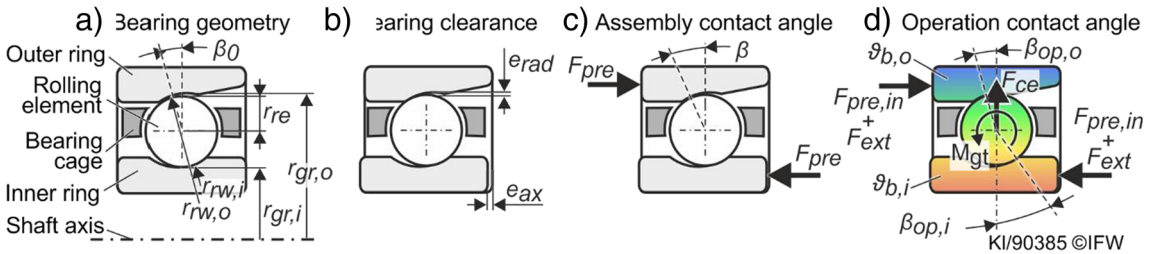

Fig. 9 Geometric properties of an angular contact ball bearing

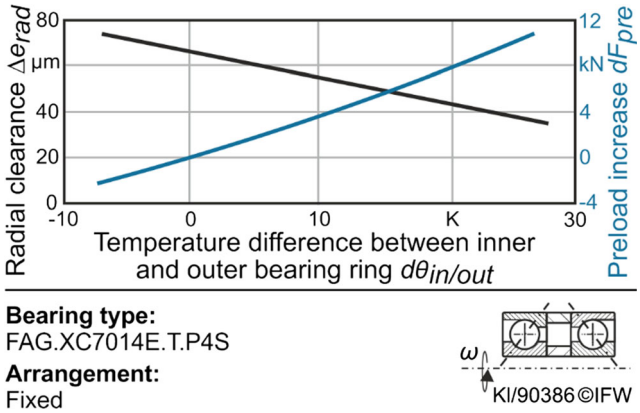

Fig. 10 Correlation between temperature difference, radial clearance, and preload according to [80]

Lowering the operating temperature of the lubricant by 10 to 15 K furthermore doubles the theoretical lifetime of the bearing lubrication [81]. In Fig. 11, the failure mechanisms according to [82] are illustrated. A stable operation of the bearing is only possible when there is an equilibrium between supplied and dissipated heat to the bearing components (green path).

With $\gamma = 3 \cdot 10^{-6}\ K^{-1}$ (silicon nitride, Si_3N_4), the coefficient of thermal expansion of ceramics is significantly lower than comparable conventional bearing materials (100Cr6, $\gamma = 12 \cdot 10^{-6}\ K^{-1}$). However, ceramic bearing rings are unsuitable for conventional motor spindles due to their comparatively low fracture toughness and high manufacturing costs. The increase in $n \cdot d_m$ values mentioned in Section 2 is instead mainly attributed to lower coefficients of thermal expansion of newly developed rolling element materials [15, 79].

Besides reducing e_{rad}, a further effect occurs when the temperature of the inner rings increases. The thermo-elastic deformation of the spindle shaft causes the inner rings to shift in axial direction relative to the outer rings. For bearings in an O-arrangement, this results in increasing e_{ax}. This effect is insignificant when the initial distances between the bearings are small. However, if this distance increases, the potential temperature-induced axial displacement increases as well. For rigidly adjusted O-arrangements, this effect leads to

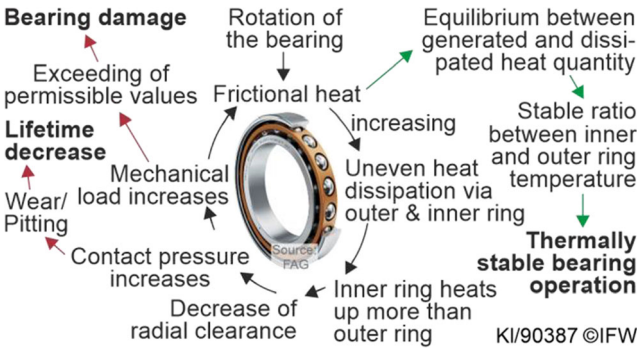

Fig. 11 Tribologically induced reduction of bearing life of rolling bearings according to [82]

decreasing F_{pre} and increasing spindle compliance. Due to the significant influence of heat on F_{pre}, bearings in spindles for very high speeds often cannot be adjusted rigidly. Such an adjustment, however, offers advantages in terms of stiffness, costs, and assembly space [50].

To reduce the thermally induced effect on the bearing preload, bearings or bearing packages are elastically adjusted. Elastic elements such as spiral or disc springs are implemented in the force flux. A disadvantage of elastic adjustment is the increase in axial compliance due to the integration of these elements. Furthermore, it is possible that axial movement may be restricted by fretting [50]. Because of centrifugal effects and the associated jamming of the bearing fits, a constant bearing preload cannot always be assured. Thus, elastically adjusted bearing arrangements can have similar properties as rigidity adjusted arrangements [77]. The effect of decreasing e_{rad} can be influenced only to a limited extent by using elastically adjusted arrangements since only the variation of e_{ax} can be compensated this way [50]. The performance limit of bearing arrangements is therefore primarily determined by the increase in preload resulting from increasing $d\theta_{in/out}$. Excessive cooling of the bearing outer rings is consequently not a suitable measure to increase the spindle performance. If cooling is too intense, e_{rad} can decrease during the operation, and thus, an increase in contact pressure is facilitated. To increase the maximum speed, the temperature rise of the inner bearing rings must be reduced. Consequently, cooling the inner bearing rings is the key to increasing spindle speed [77].

3.3 Influence of thermal load on motor performance

The motor converts electrical energy into mechanical energy. Heat is generated as a result. Summaries of detailed causes are given in [10, 83–85]. In motors, the following losses occur:

- I^2R losses (copper losses) in the stator circuit, caused by the current and ohmic resistances of the windings,
- iron losses due to induced eddy current and hysteresis losses,
- friction losses due to the overcome of tribological resistances of air,
- stray load and other losses caused by the magnetization of the conductor periphery and not purely sinusoidal supply of the motor by the frequency inverter.

In Fig. 12 (left), the proportions of these losses are illustrated for a PMM with an input power of 37 kW according to [83]. In addition to the mentioned losses, additional I^2R losses occur in the rotor circuit of IM (Fig. 12, right). I^2R losses of the stator and rotor together make up the majority of the total heat loss [83, 85]. Total power losses of several kilowatts can occur [61, 76]. Due to the I^2R losses in the rotor, the rotating spindle components are subjected to significantly higher

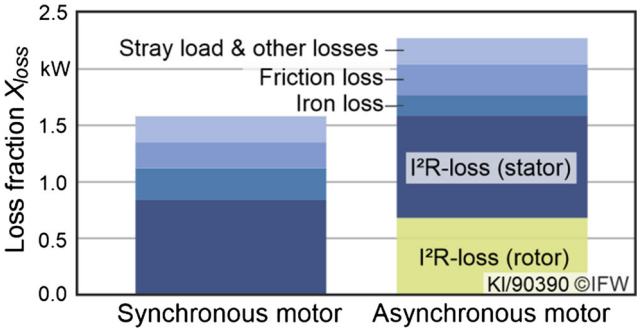

Fig. 12 Ratio of heat losses by type of loss according to [83]

thermal loads when IM are used. An increasing motor temperature resulting from these losses affects the motor efficiency negatively. In [86] it is shown that the efficiency of a PMM decreases by about 4% with an increasing permanent magnet temperature from 20 to 100 °C. In [87], the influence of the coil temperature on the efficiency of an IM with an output of 3.7 kW was investigated. A decrease of the coil temperature by 10 K results in an efficiency increase of 0.25% at 100% and 0.5% at 125% of the rated load.

According to DIN IEC 34, there are permissible maximum temperatures at the hottest spots of the winding ends. The temperature of the winding ends is the limiting thermal factor when operating a motor [88, 89]. If maximum allowable temperatures are exceeded, the motor potentially fails. High temperatures also accelerate the aging of the materials used for winding insulation. This increases the probability of motor failure [90]. The correlation between motor lifetime and maximal winding temperature θ_W is shown in Fig. 13 according to the four insulation classes of IEEE standard 117 [91]. Modern high-performance spindles usually have insulation class F.

When using PMM spindles, the rotor heats up due to heat flows from the bearings or the stator. Excessively high temperatures can lead to demagnetization and thus to permanent damage of permanent magnets. An irreversible degradation of the magnetic properties is already observed at a temperature of 130 °C [92]. High motor temperatures can therefore completely jeopardize spindle operation and result in spindle failure during operation.

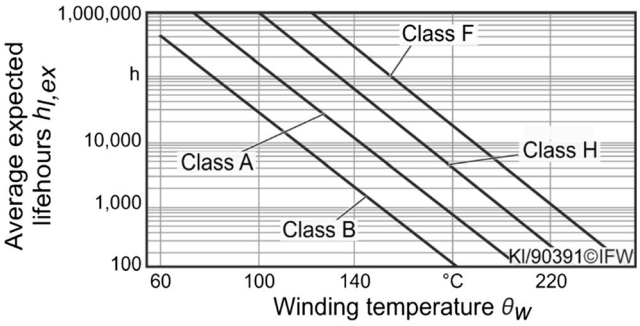

Fig. 13 Correlations between motor lifetime and winding temperature according to [91]

3.4 Influence of heat on manufacturing time

Another important factor for high precision manufacturing is the required time to achieve a thermally stable state. For the given geometry and material data, the temperature evolution $\theta_{heat}(t)$ during the warm-up period of a body can be described by Eq. 5 according to [50].

$$\theta_{heat}(t) = \theta_{stat} - (\theta_{stat} - \theta_0) \cdot e^{-\frac{\alpha \cdot A}{\rho \cdot V \cdot c} \cdot t} \tag{5}$$

The temperature development as a function of time $\theta_{cool}(t)$ during the cooling period is calculated according to Eq. 6.

$$\theta_{cool}(t) = \theta_{stat} + (\theta_{stat} - \theta_0) \cdot e^{-\frac{\alpha \cdot A}{\rho \cdot V \cdot c} \cdot t} \tag{6}$$

For simplification purposes, a homogeneous heating and cooling of the body is assumed. Heat transport by radiation is neglected. In these equations, θ_{stat} is the body temperature at the thermally stable time $t = t_{stat}$ and θ_0 is its initial temperature at $t = 0$. The convective heat transfer coefficient at the surface A of the body with the volume V, the density ρ and the specific heat capacity c is given by α.

A system is in a thermally stable state if, despite increasing time, no significant temperature variation can be observed. A commonly used value for this temperature alteration does not exist. In practice, $\Delta\theta_{lim}$ = 0.1 or $\Delta\theta_{lim}$ = 1.0 K are often assumed for the still permissible temperature change. The time t_{stat}, which is required to heat a body to a thermally stable state, can be determined by converting Eqs. 5–7.

$$t_{stat} = -\frac{\rho \cdot V \cdot c}{\alpha \cdot A} \cdot \ln\left(\frac{(\theta_{stat} - \Delta\theta_{lim}) - \theta_{stat}}{(\theta_0 - \theta_{stat})}\right) \tag{7}$$

Here, $\Delta\theta_{lim}$ is the individually definable value of temperature changes that are still permissible. In Fig. 14 (top), an exemplary heating and cooling sequence for a C45 shaft with a diameter of 50 mm and a length of 300 mm is shown. The

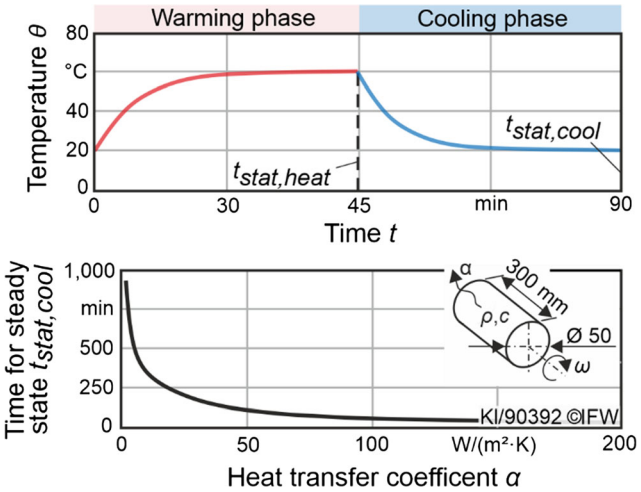

Fig. 14 Influence of convection on the time to reach a thermally steady state

shaft is heated from an initial temperature θ_0 = 20 °C to θ_{stat} = 60 °C. Forced convective heat transfer caused by rotation is assumed with α = 100 W/(m^2·K). According to Eq. 7, a time of about 45 minutes is obtained for heating and cooling when a temperature limit value of $\Delta\theta_{lim}$ = 0.1 K is assumed. The required times are significantly influenced by the value for α. In Fig. 14 (bottom), the effect of varying α on the time required to reach a thermally stable state is shown. If α is doubled, the required time for cooling $t_{stat,cool}$ is halved. From these correlations, it becomes clear that the required time to reach a thermally stable state depends on the temperature difference $\theta_{stat} - \theta_0$. The greater this difference, the longer the time required to reach a steady state. Moreover, this time increases if the amount of heat dissipated convectively from a system decreases. Consequently, an increase in cooling performance enables an earlier achievement of a thermally stable state.

To reduce the influence of instationary heat flow, warm-up cycles are often used in practice [33]. The spindle rotates at defined speeds according to a specified speed-time profile. Machining of the workpiece does not begin until the warm-up phase has ended. The higher the spindle temperatures, the longer the warm-up cycle required to achieve a stable state. This in turn reveals that the level of the resulting temperature has a significant influence on the non-productive time of a manufacturing process.

4 Cooling concepts for motor spindle components

A large number of cooling strategies are available to reduce undesired effects due to thermal loads. The following section provides an overview of cooling concepts that have been developed or considered in recent decades. A distinction is made between motor (4.1), bearing (4.2) and shaft cooling (4.3) concepts. However, it must be noted that due to thermal coupling of spindle components, variations of local temperatures of one component inevitably also influence the temperature field of other components [2].

4.1 Cooling of spindle motors

The existing concepts for cooling spindle motors differ considerably in terms of their operation principle. In the following, a distinction is made between passive (Section 3.1.1) and active (Section 4.1.2) approaches. Passive approaches are measures in which the body being cooled is not directly cooled by an externally applied cooling media. In active approaches, a cooling media is directly applied in such a way that a corresponding reduction of the target body temperature is achieved.

4.1.1 Passive motor cooling

Cooling solely by passive measures is conceivable, especially for small motors with low torque and low bearing friction losses (e.g., dressing or grinding spindles). In such cases, the effect of convection to the surrounding air is often sufficient to achieve a sufficient cooling effect. The cooling effect can be augmented by increasing the surface area of the spindle housing or by adding lamellar structures to the housing [93]. Due to the low heat transfer capacity of air and the prevalent laminar flow conditions, however, the achievable temperature reduction is minor [94]. Due to the high thermal load on the winding ends, measures to reduce these loads are usually implemented already during the design phase of a motor. Such a measure is the optimization of the winding cross sections and winding number to reduce winding losses. In addition, the stator slots and the winding ends can be thermally coupled to heat sinks (e.g., cooling channel sleeves). The heat transfer from the motor core can also be increased by applying casting compounds with heat-conducting fillers and high dielectric strength (e.g., powdered aluminum nitride). Another passive measure is the use of thermally optimized sheet materials [10].

Heat transport also occurs throughout the motor air gap. This heat transfer has a significant influence on the temperature within the drive [10]. Since the rotor of IM usually exhibits higher absolute temperatures, heat is transferred from the rotor to the stator. In the case of PMM, the heat transfer can also occur inversely due to the generally lower rotor temperature [95]. The heat transfer between the rotor and stator increases significantly with increasing motor speed. Reducing the air gap width from 0.6 to 0.3 mm only leads to marginally increasing heat transfer [10]. With small air gap widths, however, additional losses are caused which increase with the product of the number of stator slots and rotational speed [96]. Measurements carried out on a 7-kW IM spindle with a maximum speed of 36,000 min^{-1} revealed that by increasing the air gap width from 0.175 to 0.350 mm, additional losses can be reduced by more than 5% during idling and by more than 10% under load conditions. Consequently, there is an optimum between the hysteresis losses resulting from remagnetization and the current heat losses [10].

Heat losses can also be influenced by the type of supply. During motor operation, magnetization losses occur in the iron as a result of magnetic fluxes with frequencies of the voltage harmonics and harmonics with the switching frequency of the inverter. In [97], it is shown that these losses can be decreased by reducing the switching frequency and inverter input voltage. When operating at rated power, on the other hand, the total motor losses decrease with increasing switching frequency of the inverter. The waveform of the voltage curve is more favorable regarding the overall motor losses. The low-order harmonics, which propagate significant currents, become smaller. Particularly in the rotor, current

displacement effects do not have as much effect in this case. In [98], the effect of supply pulses on the temperature field of a PMM spindle with a maximum power of 17.5 kW and a maximum speed of 54,000 min^{-1} is investigated. A three-point inverter with 64 kHz, a two-point inverter with 8 kHz, and a two-point inverter with 16 kHz switching frequency are considered. When supplying with the two-point inverter (8 kHz), temperatures of up to 100 °C occur in the rotor. When supplied with the three-point inverter, only approx. 45 °C is attained. In [10], current and voltage waveforms of different frequency inverters are compared with each other. Compared with an optimal sinusoidal supply, supplies with PWM, PAM, and PAM-PWA signals lead ascendingly to increasing heat losses in the rotor. The resulting increase in motor performance, however, is at the expense of decreasing efficiency. The effect of the supply on the thermal load on the spindle can, however, be improved by using suitable filter techniques. Such an approach has been patented in [99]. However, a quantitative evaluation of this principle is not known. Such supply-technical approaches for decreasing heat losses are technologically largely depleted nowadays. The acquisition costs for required high-performance converters are, however, high. Therefore, mostly less performant but inexpensive converters are used in practice.

A variety of passive cooling concepts for cooling conventional electric IM using heat pipes can be found in the literature. Heat pipes are evacuated pipes containing a certain amount of a liquid (usually deionized water). This liquid evaporates at the warmer end of the pipe and then condenses at the colder end. As a result, heat is removed from the evaporation area. The condensed liquid is returned to the location of higher temperature by gravity, capillary, or centrifugal forces. The thermal conductivity of heat pipes can be up to several potencies higher compared with a geometrically similar, metallic conductor [10]. Such approaches can be found in [100–107]. In [105], a concept with 36 heat pipes in the stator of a conventional IM is analyzed. The motor power loss of the stator and rotor is 7.5 kW and 3.5 kW, respectively. The heat transferred through the heat pipes is convectively dissipated by an air-cooling device. In comparison to an identical air-cooled motor, the winding temperature could be decreased from 90 to 40 °C. In [104], a concept for cooling a conventional IM based on eight L-shaped heat pipes embedded in the stator is presented. As heat sinks, lamellar heat exchangers are mounted on the ends of the heat pipes. The heat exchanger convectively dissipates the heat at the rear end of the motor housing. This approach reduces the surface temperature of the housing from 102.2 to 68.4 °C at a thermal motor load of 150 W. However, cooling of machine tool spindle stators using heat pipes is not known. A reason for this is that conventional electrical motors are frequently used in stand-alone applications. Cooling of motor spindles can generally be achieved comparatively simply and efficiently by using obligatorily existing auxiliary cooling units instead. A passive approach for cooling the motor of a spindle is presented in [108, 109] by integration of thermoelectric Peltier elements. A Peltier element is an electro-thermal transducer that generates a temperature difference when a current flows or generates a current flow when a temperature difference occurs. In preliminary tests, the temperature of a reference measuring point could be reduced from 64.3 to 41.5 °C at a heat load of 200 W [108]. These modules also allow temperature control in case of changing induced heat flow rates.

Passive approaches generally have low operating and maintenance costs. In addition, no additional energy or resources are required. Additional space required for the integration of these concepts is not necessary or is marginal. However, the main disadvantages of passive concepts are the comparatively low cooling effect and limited adjustability of the cooling performance. Due to the small amount of heat that can be dissipated, active cooling measures must be applied to spindles with high thermal loads.

4.1.2 Active motor cooling

For active cooling, the use of water with anticorrosive additive is particularly widespread. However, air and oil are also used as cooling liquids [110]. The amount of heat that can be dissipated by a flowing liquid $\dot{Q}$ is determined by Eq. 8.

$$\dot{Q} = c \cdot \rho \cdot \dot{V} \cdot \left(\theta_{fluid,out} - \theta_{fluid,in}\right) \tag{8}$$

Thereby, $\theta_{fluid,out} - \theta_{fluid}$ is the difference between the temperatures of the inlet and outlet flow of the fluid. The flow rate $\dot{V}$ is the product of the fluid flow cross-section A_{fluid} and the average flow velocity v_{fluid}. Water-based cooling is generally more effective due to its higher specific heat capacity [10, 111]. With a value of 41.2 kJ/(kg·K) at 20 °C, it is significantly higher than the heat capacity of air (1.005 kJ/(kg·K)) or special cooling oil (~ 1.9 kJ/(kg·K)). Nevertheless, the application of cooling oil is particularly popular in the warm and humid Asian area. This is due to the oil's lower susceptibility to microbial contamination.

Air-based cooling of motor spindles is only applied if the occurring heat losses are low [110]. These systems are particularly attractive for applications with high-cost constraints due to their comparatively simple design and easy maintainability. An advantage of air-based cooling systems is a considerably lower requirement for space of peripheral equipment (e.g., cooling unit). In [112], a concept for cooling a motor spindle by means of a wide jacket cooling flow is proposed (Fig. 15a). The air flows around lamellar sheets of the stator. Although this cooling concept was implemented industrially [115], it was later enhanced by water cooling due to low heat dissipation [116]. In [113], active cooling of a motor spindle housing is achieved using a fan mounted at the rear end (Fig. 15b).

This fan supplies ambient air from the spindle rear to the front through axial ducts in the spindle housing. With this concept, the temperature at the rear can be significantly reduced. However, as the air warms up, the cooling effect on the front area of the housing is small. In addition, this approach leads to an increased acoustic pollution due to turbulent airflow. With the knowledge that a turbulent flow improves the heat transfer properties of fluids, an approach was researched in [114] that took advantage of the Coandă effect (Fig. 15c). This effect describes the induction of a secondary fluid flow through the flow of a primary fluid flow. A perforated silicone tube is placed at several points around the spindle housing and compressed air is passed through. With this approach, the thermally induced spindle growth can be reduced by about 30%. However, a considerable airflow rate of up to 200 l/min is required to achieve this effect.

In [117, 118], liquid-based approaches for cooling a PMM with a rotor diameter of 11 mm and a maximum speed of 280,000 min^{-1} are researched. By introducing 12 axial channels between the stator windings, the winding temperatures can be reduced by about 60%. By implementing a water-based annular gap cooling between the stator windings and the air gap, the temperature is reduced by about 70%. If the winding temperature is limited to 80 °C, this approach can achieve a performance increase of about 100%. In [119], the sheet metal plane of a stator stack is cooled by a fluid flowing through channels. This approach reduces heat generation in the stator by approx. 80%. Already in [10], such an approach for cooling of spindle motor winding ends is described as conceivable. These attachments provide a high potential for cooling. However, design effort and associated additional costs for such cooling systems are high. For this reason, closed cooling circuits with circulating liquids are widely used for the active cooling of spindle motors nowadays. The stator is cooled from the outside by means of a jacket flow (Fig. 16). The design and manufacturing of jacket cooling systems is comparatively simple. Due to the immediate proximity to the stator, heat can be dissipated sufficiently. An optimal thermal coupling of the cooling channel sleeve to the stator is important.

Apart from chemical or physical properties of the fluid as well as the flow velocity, the maximum dischargeable amount of heat depends on the geometric properties of the cooling channel. The height and width of the flow cross-section and its curvature have an influence [10, 110]. The heat transfer from the cooling channel wall to the fluid is also influenced microscopically by surface properties [10, 120, 121]. Many investigations of the geometric aspects of the cooling channels have been carried out as they offer a wide range of optimization potential (e.g., [80, 121–133]. In these studies, efforts are made to improve the efficiency of cooling by optimizing the macro- and micro geometry of the cooling channels. A fractal arrangement of cooling channels in the spindle housing results in a cooling efficiency about two and a half times higher than with spiral channel geometry [129]. The pressure to be applied to transfer the fluid can also be reduced several times by a fractal arrangement. In [121], the influence of the surface roughness of the cooling channels is investigated. It is found that the heat transfer coefficient between cooling body and fluid can be more than doubled if a mean roughness depth of Rz = 100 µm is applied instead of an ideally smooth surface. Effects of flow velocity are investigated in [134]. It is found that the effect of v_{fluid} on the resulting temperature decreases regressively with increasing v_{fluid}. However, this effect is no longer significant at velocities of $v_{fluid} > 1.5$ m/s.

Active measures generally require more energy as a result of additional or larger aggregates. This also implies potentially higher acquisition and maintenance costs as well as additional space requirements. Moreover, additional design modifications are necessary, e.g., for the integration of cooling channels. Nevertheless, active cooling of spindle motors is the most common method for heat dissipation due to its superior cooling performance.

4.2 Cooling of bearings

Whether bearings need to be specifically cooled depends on the application-specific requirements of the spindle. Bearings are not cooled if sufficient spindle functionality can be

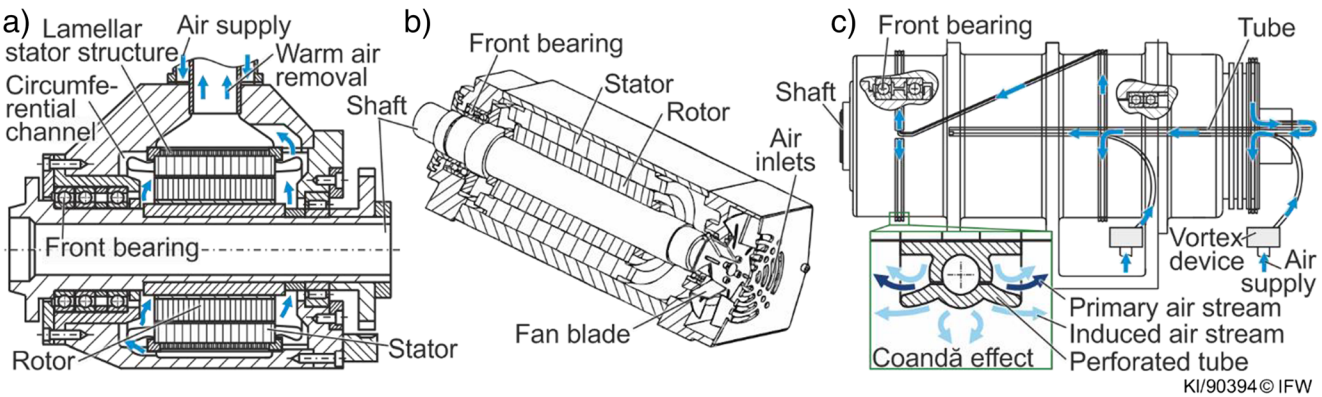

Fig. 15: Air-based concepts for cooling spindles. Jacket cooling a) [112], fan cooling b) [113] and Coandă effect c) [114]

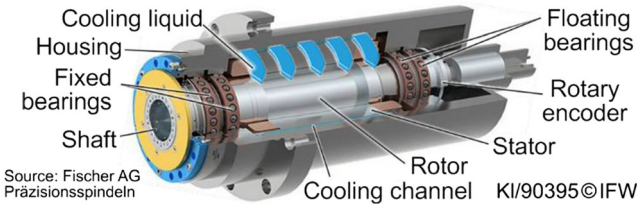

Fig. 16 Jacket cooling of a modern motor spindle

expected despite the occurring temperatures. In these cases, the heat dissipation due to heat transport through thermally coupled components or by convection is sufficient. In addition, there is always a self-cooling effect of the bearings through convection during rotation. This effect is particularly noticeable if the bearings rotate at high speeds [8]. The elimination of an additional cooling structure reduces spindle manufacturing costs.

Bearings can be passively protected from thermal influences of the motor by heat shields or labyrinth seals (Fig. 17). In some cases, heat shields are additionally provided with cooling channels [10]. However, since bearing inner rings are thermally indirectly coupled to the motor by the spindle shaft, such measures do not provide complete thermal protection.

The bearing and motor heat losses occurring during operation of modern high-performance spindles are often considerably high so that active cooling is required. The cooling of the bearing outer rings by liquid flowing through the spindle housing is the most commonly used cooling technique [8]. In practice, the front spindle housing is kept at a definable temperature. The primary objective of cooling the bearing on the housing side is to reduce the time required to achieve a stationary temperature field. Targeted cooling of the rear bearing is often not required, since the heating of the rear spindle section usually has only minor influence on the time required to reach a thermally stable state.

A further possibility for actively reducing the bearing temperature is the adjustment of lubrication parameters. For high-speed spindles, oil-air lubrication is often used. An airflow is injected through a nozzle between the inner and outer ring of the bearing. The airflow carries small oil droplets. The oil is previously discharged from a lubrication unit into the airflow in definable

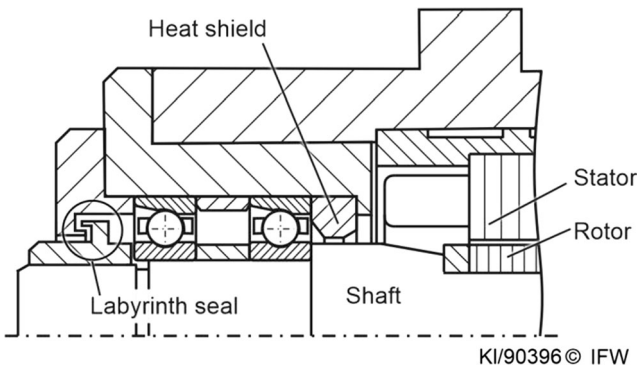

Fig. 17 Example for an application of a heat shield

time intervals. Wu et al. [135] and Li et al. [136] examine the effects of lubrication parameters on the temperatures of high-speed bearings. In these studies, it is shown that the outer ring temperature of an oil-air-lubricated bearing can be reduced by about 5 K by reducing the oil flowrate from 0.08 to 0.02 ml per lubrication cycle. An increase in the lubrication interval from 2 to 10 min leads to a quantitatively comparable temperature decrease. By increasing the air pressure from 0.3 to 0.5 MPa, the temperature of the outer ring can be decreased by approx. 4 K. By increasing the oil viscosity from 15 to 68 cSt, a quantitatively similar effect is achieved. In [137] these variables are also varied at a spindle speed of 30,000 min^{-1}. By increasing the pressure from 0.29 MPa to 0.41 MPa, a reduction of $d\theta_{in/out}$ of about 30% can be achieved. A quantitatively similar effect is achieved by increasing the lubrication interval from 0.2 to 90 s. However, the effects of such bearing lubrication manipulations on the long-term operation of the spindles are not investigated in these papers. The reduction of bearing temperature by variation of lubrication parameters is economically interesting as no additional equipment and maintenance costs occur. Nevertheless, the achievable cooling effect is comparatively low.

A common method for active cooling of bearing is indirect cooling by cooling the spindle shaft (see Section 4.3). However, concepts in which the bearing inner rings are cooled directly also exist. In [139, 138], a ring-shaped spacer is described by which an oil-air-flow is guided onto the bearings (Fig. 18). A similar concept was patented already in 1965 [140]. The spacer is installed between two bearing outer rings. Hereby, $d\theta_{in/out}$ could be reduced by about 40% at a speed of 23,000 min^{-1}. With undercooled air, it was even possible to achieve negative values for $d\theta_{in/out}$ at lower speeds. A disadvantage of this concept, however, is the high demand for air and a significant increase in the noise level. In addition, sufficient air cleanliness must be ensured to prevent contamination of the bearings.

In general, the cooling of high-speed rotating components by airflow is only effective to a limited extent. With increasing relative velocity between rotating surfaces and the surrounding air, the impulse force of the air particles within the boundary layer of the rotating surface increases. As a result, an air jet directed at a rotating surface is tangentially deflected. Consequently, the cooling effect decreases with increasing rotational speed [141].

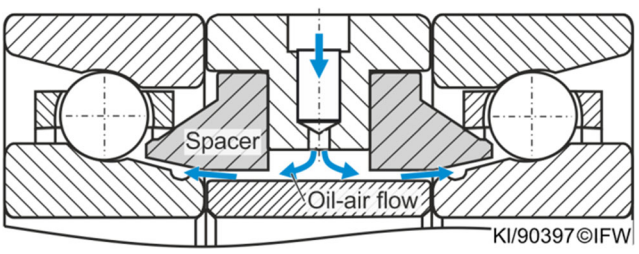

Fig. 18 Oil-air cooling by spacer [138]

4.3 Cooling of spindle shafts

As already described in Section 3, a temperature increase of rotating components leads to a variety of undesired effects. In particular, the stiffness and the achievable maximum rotational speed are limited. In O-arrangements, the preload generally increases as a result of a temperature rise of the inner rings and the shaft. This preload change must already be taken into account during the design phase of a spindle. For this purpose, the initial bearing preload is initially reduced so that a certain preload limit value is achieved under maximal thermal and mechanical load. As a result, spindle compliance is increased over a wide operating range especially at lower speeds. By cooling the shaft or the bearing inner rings, a higher initial bearing preload and thus a lower compliance of the shaft-bearing-system can be achieved. It is also possible to achieve a higher maximum speed with the same or even higher initial bearing preload. These correlations can be seen qualitatively in Fig. 19. The cooling of the shaft is therefore an effective measure to increase the performance of spindles. An example of a passive design approach for cooling spindle shafts is the application of labyrinth seals proposed in [10] (Fig. 17). Their primary purpose is the protection against contamination of the spindle. However, the design of the air gap geometry can also be used to improve the heat transfer from the rotating system to the housing [10]. Nevertheless, a quantitative evaluation of the cooling effect of labyrinth seals is not known. Another passive approach for cooling of rotating shafts is the application of heat pipes. Before concepts for the integration of heat pipes in motor spindles were considered, a number of similar approaches for cooling conventional electric motors were developed (Fig. 20). There is a series of studies and patents in which heat dissipation is achieved by means of lamellar heat exchangers rotating with the shaft [100, 105, 142–149]. In the patent application [143], an approach is shown in which a heat pipe is inserted in the middle of an electric motor shaft (Fig. 20a). In [95, 150–154], the shaft has fluid-filled cavities. This eliminates the actual heat pipe wall and thus additional

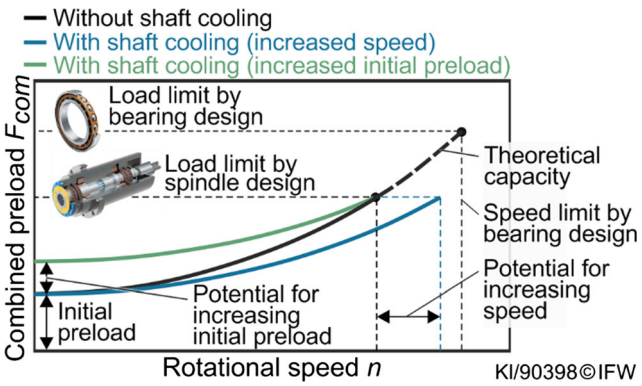

Fig. 19 Qualitative illustration of the influence of shaft cooling on the performance increase in spindles

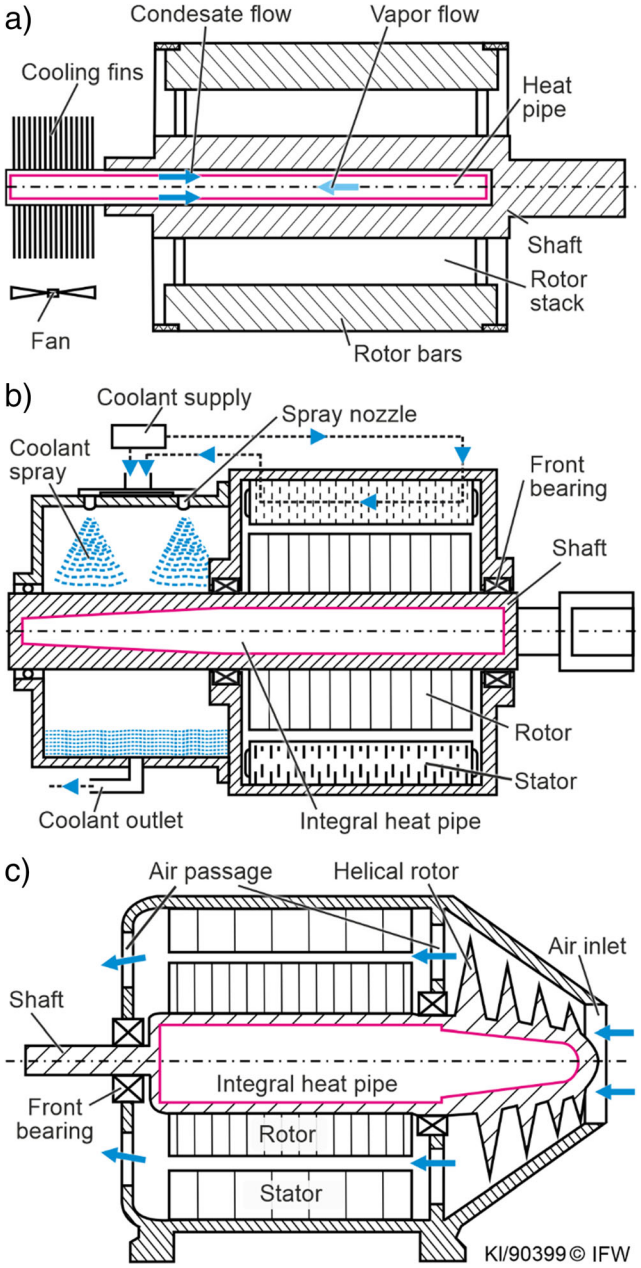

Fig. 20 Cooling of motors by applying a heat pipe in the center of the shaft. Heat sink by **a** rotating fins [143], **b** spray cooling [152], and **c** helical cooling structure [150]

thermal resistances. In [152], cooling occurs within a spray chamber sealed towards the motor. Coolant is sprayed directly onto the shaft by a nozzle (Fig. 20b). In [150], a helical structure serves as a heat sink that conveys air through the engine during rotation (Fig. 20c). This allows the available motor power to be increased by 15 % without an increase in winding temperature. An approach combining a helical structure and cooling fins on a motor shaft can be seen in [155]. In [151], disc-shaped fins are installed at the front end and a fan at the rear end of a motor. In the rear end, air is blown onto the shaft. Hereby, a motor with a maximum speed of 13,500 min^{-1} and

a rotor power loss of 44 W is cooled. The rotor temperature can thus be reduced from 130 to 98 °C.

Such shaft cooling systems were mainly developed or conceived in the 1970s and 1980s and later transferred to applications in motor spindles. Judd et al. [156] investigated the use of heat pipes for bearing cooling within the center of a machine tool spindle shaft at a maximum rotational speed of 2,778 min^{-1}. The condensation zone of the heat pipe was cooled with ice and water. A temperature decrease of around 50% was achieved. The cooling effect was found to be negligible when environmental air was used instead. In [157], an annular heat pipe within a shaft axis is used (Fig. 21a). The heat pipe has inclining condensation zones using centrifugal forces to support fluid return to the evaporation zone. With this approach, the maximum shaft temperature was decreased by around 40% at a maximum speed of 24,000 min^{-1}. In [42, 158] a spindle with several eccentrically rotating heat pipes in the spindle shaft is presented and investigated experimentally. The maximum temperature of the spindle could be reduced by 35%. In [159, 160] the same authors present an alternative approach in which a cavity of straight holes connected to each other by annular channels and radial holes is manufactured into the spindle shaft. This cavity is filled with fluid and is evacuated afterwards. The experimental results in [160] revealed a temperature decrease of the heat pipe evaporation section from 99 to 57 °C (− 42%) for a heating load of 150 W and at a rotational speed of 1,000 min^{-1}. An arrangement of several eccentrically rotating heat pipes is also suggested in the utility model [161] (Fig. 21b). Several heat pipes eccentrically rotate within a gear-driven spindle. Between the bearing locations, a lamellar cooling structure is located as a heat sink. A cooling medium is streaming onto a lamella structure through openings in the housing. A technological evaluation of this concept is not known. A further implementation of a combination of heat pipes and lamellar cooling structures can be seen in [27] (Fig. 21c). Here, 15 heat pipes rotate in the front area of an IM spindle shaft. The considered spindle has a maximum power of 11 kW. Heat is transported from the front bearings to a fin-shaped heat exchanger in the middle of the bearings. Heat from the motor and from the rear bearing is conducted to a second heat exchanger system through further eight heat pipes in the rear of the shaft. Contrary to the previously mentioned concepts, however, non-rotating fins coupled to a heat sink are used in this concept. Heat is transferred from the rotating fins through an air gap of 0.2 mm (front) and 0.3 mm (rear). The heat is finally dissipated from the system by conventional jacket cooling. As a result, spindle growth can be reduced by 47% at a speed of 20,000 min^{-1}. The temperature difference $d\theta_{in/out}$ of the fixed bearing close to the motor is reduced by up to 66%. In addition, the time required to achieve a thermally stable state is reduced by an average of 56%. The latter concept does not require an additional coolant supply, which must be sealed separately.

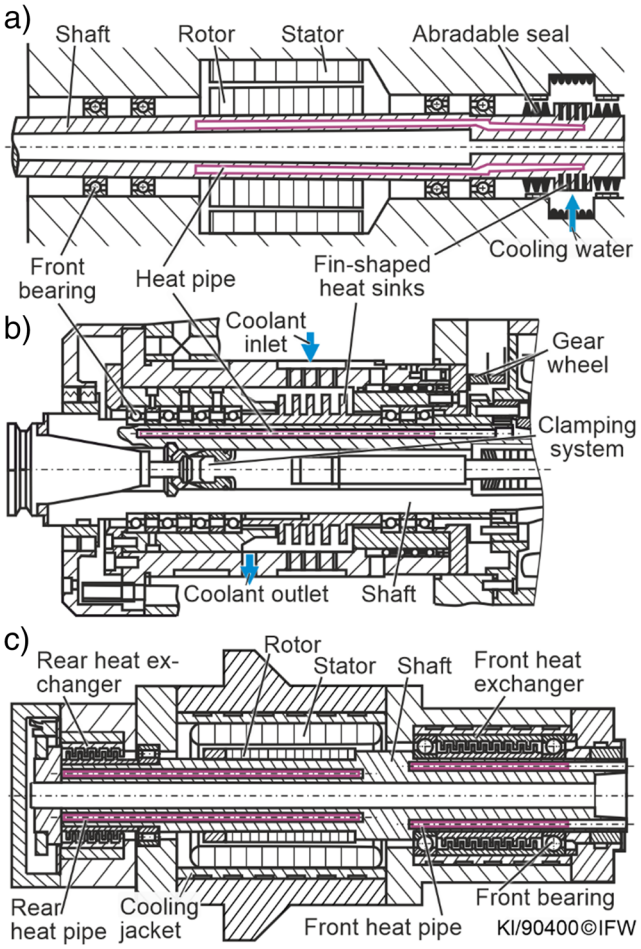

Fig. 21 Concepts for cooling of spindle shafts with heat pipes according to **a** [157], **b** [161], and **c** [27]

Although a significant decrease of thermal load is possible through the introduction of heat pipes, such cooling concepts are not known in commercially available spindles. The reason for this are high costs due to required deep bores [162]. In addition, the achievable cooling capacity is still low compared with liquid-based concepts.

The described passive cooling measures provide particular economic and ecological advantages. Due to the absence of additional aggregates, the operating and maintenance costs of these approaches are low. However, the cooling performance and cooling adjustability of these approaches are low compared with active concepts. Active shaft cooling systems are applied when the expected heat load is particularly high or a particularly high manufacturing accuracy is required. Cooling is achieved by a fluid flowing through the shaft. The fluid is therefore fed through a rotary joint into one or more cooling channels within the shaft. There are also rotary joints that are simultaneously used to feed cooling lubricants into the process zone through the shaft. In Fig. 22, the design of such a three-channel feedthrough is shown. The heated liquid is conveyed through the rotary joint or through an outlet in the spindle housing back into the cooling unit. In the patent

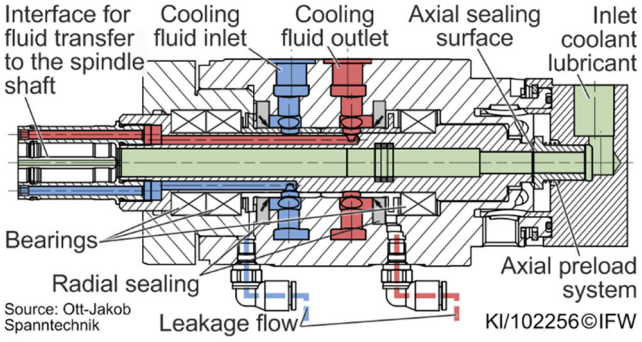

Fig. 22 Assembly of a three-channel rotary feedthrough

specifications [163] (Fig. 23a) and [164], it is suggested that a cooling fluid circulates through a threaded groove on the shaft surface. In [165], this concept and its cooling effect, necessary cooling oil pressure and the sealability by air seals is investigated using fluid simulations. In this study, a modified cooling concept is also investigated. Only the front area of the spindle between the bearings is cooled (Fig. 23b). Axial bores are located in the shaft through which the cooling oil passes. This concept is also investigated in [166] with regard to its cooling effect and is patented in [167]. Through this approach, a decrease of spindle elongation by about 50% and a decrease of the time to reach a thermally stable state by about 80% is achieved with an oil flow rate of 3 l/min. However, in [165], it is stated that this concept is clearly susceptible to leakage and bubble generation in the cooling oil. In addition, a significant increase in oil pressure required for cooling is necessary with increasing speed. The utility model [168] presents a similar concept. Here, however, cooling is done using gaseous media. By means of gap seals, a pressure gradient is built up in the front area of the spindle. This leads to a through-flow of the shaft bores below the fixed bearings. However, an evaluation of this approach is not known. In [169, 170] a concept is described in which the spindle shaft is provided with several axial cooling channels. The cooling fluid is fed into the shaft by means of a rotary joint integrated into the spindle. This concept allows the dynamic compliance of a 13.5 kW spindle with a maximum speed of 42,000 min^{-1} in radial and axial direction to be reduced by 16% and 70% respectively.

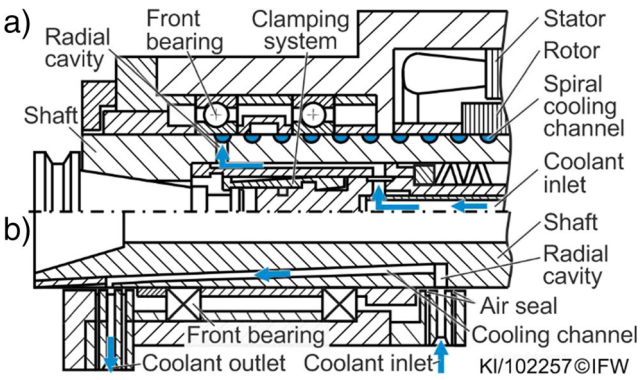

Fig. 23 Shaft cooling according to [163] (**a**) and [165, 167] (**b**)

However, in this article the rotary joint is evaluated as a "critical key component" due to leakage. In [80, 171], a similar shaft cooling principle is presented based on the patent in [172] (Fig. 24a). By reducing the temperature difference between the inner and outer rings of an angular contact ball bearing pair (7014E, O-arrangement), e_{rad} under load is significantly increased [80]. It is pointed out that implementing a rigidly preloaded arrangement by applying this cooling concept is possible. In [171], the effects of cooling on the performance increase of a motor are described. Increased torques are achieved by an electrically favorable design of the sheet metal sections. The resulting higher thermal load on the rotor is reduced by means of shaft cooling. The necessary length of an IM in relation to the torque is thus only 15% higher than the required length of a PMM with a comparable torque of 800 Nm. Cooling of the shaft also reduces the total thermal growth of the spindle by about 70%. In the patent specification [173], an approach is shown in which oil is passed through the spindle shaft (Fig. 24b). The temperature-controlled oil not only acts as a coolant, but also lubricates the bearings simultaneously. The oil is guided through small bores in the bearing inner rings into the bearing contact zone. Centrifugal forces during rotation facilitate this transport. Using this concept, $d\theta_{in/out}$ can be controlled. This technology is used to equip motor spindles with particularly high thermal stability requirements. The spindle housing is cooled by a second cooling circuit, but with the same oil. A disadvantage of this concept

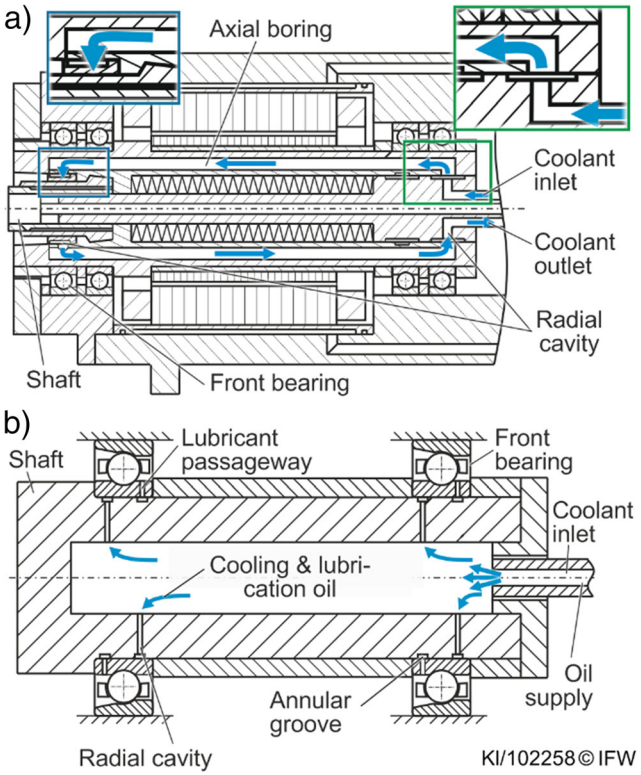

Fig. 24: Liquid-based concepts for spindle shaft cooling according to [172] (**a**) and [173] (**b**)

is the susceptibility to clogging of the lubrication channels in the bearing inner rings by microscopic metal particles in the oil. These particles can, for instance, contaminate the fluid circuit as a result of a spindle crash. Moreover, the required bearings with bores are expensive custom-made products.

Shaft cooling involving liquid media provides high cooling performance. The adjustability of the cooling capacity is likewise high. Nevertheless, there is a number of disadvantages associated with these concepts, e.g., necessary expensive deep drilling operations for the channels. Bubble generation in the coolant flow can cause the shaft to become unbalanced during operation. In addition, such concepts are susceptible to leakage. Especially at high relative speeds between seal and sealing surface, the sealing of rotary joints is difficult for dynamic reasons [10]. At low relative speeds between seal and sealing surface, highly viscous liquids, in particular oil, are used. Due to the high viscosity, the leakage flow can be reduced. However, machine cooling systems are often operated with water-based liquids. As a result, an additional oil unit may be required to cool the spindle shaft. The required energy of such aggregates is considerable [174]. Depending on the design of the rotary joint, liquids with a lower viscosity are required at higher relative speeds. Otherwise, the required feed pressure may increase significantly [165]. However, the lower viscosity leads to an increased leakage flow. Leakage from rotary unions is the second most common source of failure when operating spindles [175]. As a result, the operation of rotary joints can only be ensured by time-consuming maintenance work, which results in machine downtime. Due to the complex design of fluid-based shaft cooling systems and required peripheral equipment, the costs of these systems amount to approximately 15–30% of the total spindle costs.

5 Future challenges

Irrespective of the cooling concept, a basic distinction can be made between:

- spindles with devices for cooling the stator,
- spindles with devices for cooling the stator as well as for temperature control of bearing outer rings, and
- spindles with additional liquid-based cooling of the shaft.

The extent of cooling measures depends on the application-specific accuracy requirements of the spindle. If requirements are low, the cost advantages of a spindle without a complex cooling system prevail. The technological benefit achievable with a cooling system is then deliberately neglected. Commercially available modern high-performance spindles, which are not equipped with fluid-based shaft cooling, generally have no device for targeted cooling of the shaft or the bearing inner rings at all. However, there is also a series of scenarios in which the requirements for manufacturing accuracy are neither very low nor very high. In such cases, the question of the necessity of targeted shaft cooling from a monetary point of view is often not easily answered. Due to the high acquisition and follow-up costs of liquid-based shaft cooling systems, decisions are often made not to additionally cool the shaft in such cases. In marginal situations, however, a non-existent shaft cooling can threaten the process ability of the spindle. In such cases, the process parameters are softened to reduce thermal loads. The theoretically available spindle power is not utilized. The result is decreasing productivity. Machine tool users must therefore calculate very precisely whether the current and future economic situation requires and permits the acquisition of a spindle with cost-intensive cooling. Consequently, there is a technological-economic deficit between cost-effective cooling systems based on jacket cooling and systems with liquid-based cooling of the spindle shaft. In the future, this deficit will have an even greater impact on manufacturing practice. In Sections 2 and 3, two significant trends in manufacturing practice became apparent: Demands for accuracy of the workpieces to be manufactured are increasing (Fig. 1). However, a continuing trend towards increasing power density and increasing maximum speed is observed (Fig. 3). Taking into account the correlations shown in Section 3, a corresponding conflict of objectives between increasing machining accuracy, process efficiency, and increasing thermal loads on the spindle is evident. As a result, increasing technological potential for improving the efficiency of manufacturing processes cannot be exploited due to limiting thermal effects.

If manufacturing accuracies are to be maintained despite even higher thermal loads, it is necessary to modify the design of modern high-performance spindles and their operating strategies. Essential instrument therefore are optimizations and new developments of concepts for the cooling of thermally exposed spindle components. Due to the increasing power losses of the motor, efficient concepts for the cooling of stator and rotor must be further developed or brought into industrial practice. To achieve higher speeds and higher initial bearing preloads, spindle bearings and bearing concepts must be optimized. The optimization of bearing cooling is an important factor in this respect. Increasing the cooling capacity in the area of the bearing outer rings, however, is not an appropriate approach. Instead, reducing the temperature differences between the bearing inner and outer rings must be achieved. The most promising approach for reducing the temperature difference is the cooling of the shaft and bearing inner rings. In Section 4, existing and conceivable approaches were presented. For commercial applications, however, only complex approaches based on fluid cooling are known. Alternative concepts exist but they reveal significant deficits regarding achievable cooling performance, costs as well as energy and resource efficiency. Consequently, cost-effective alternative concepts for cooling the spindle shaft or the bearing inner rings

must be developed. Therefore, the technological-economic deficit between shaft-cooled and uncooled or outer-ring-cooled spindles has to be narrowed or completely removed.

6 Summary

Technological advances in the fields of bearings, lubrication, and the development of more powerful and efficient motors have led to widespread market penetration of motor spindles with roller bearings. Today, there are noticeable trends towards higher maximum speeds and motor power. Due to increased power density of motor spindles, heat losses within the spindle increase. These losses can cause a number of undesired thermal, thermo-mechanical, and tribological effects. As a result, the process capability of a spindle and thus the productivity of a process can be reduced. To operate modern high-performance spindles, it is therefore necessary to provide systems for cooling thermally exposed spindle components. The measures to be taken and their extent depend on the process-specific requirements of the spindle system. In addition, there are various motives for the development of cooling systems. These include the need to keep absolute temperatures of the temperature field low. The minimal temperature difference between the inner and outer ring of a bearing must also be considered it is crucial to achieve higher speeds and implement more powerful motors. These motives have led to research and development of a series of concepts for cooling spindle components in recent decades. Such concepts were presented in this article. The aspects explained as well as the most significant conclusions are summarized in the following:

- A distinction was made between the cooling of motors, bearings, and spindle shafts. In each case, a distinction was made between passive and active approaches.
- It can be stated that passive measures have clear advantages with regard to their acquisition and operating costs as well as their resource efficiency. However, active cooling concepts have become established in industrial practice due to their fundamentally higher cooling potential.
- Fluid-based cooling systems with a closed cooling circuit are widely used. These systems are used both for cooling the stator and the bearing outer rings and for cooling the rotor as well as the bearing inner rings. Indirect cooling of these components by means of cooling channels in the shaft is widely applied.
- Fluid-based shaft cooling systems are only used in cases where particularly high demands are placed on process stability and spindle reliability. High costs for these concepts account for this. These costs can amount to up to 30% of the total cost of the spindle system. For this reason, the majority of spindles on the market do not have shaft cooling systems.
- If a spindle is not equipped with a shaft cooling system, the rotating components of a spindle are not specifically cooled. Such cooling is, however, necessary to fully utilize the potential of modern high-performance spindles. As a result, the performance of a number of such spindles today is limited by the absence of the cooling of rotating components.

In the future, it is probable that, as a result of the trends towards higher spindle speeds and motor power, raising the performance potential of spindles will not be possible due to insufficient cooling of the rotating components. In recent years, there has been a significant increase in research and development activities in the field of spindle cooling. However, efficient and more cost-effective cooling concepts for the rotary components must be developed and put into industrial practice.

Authors' contributions Not applicable for that section.

Funding Open Access funding enabled and organized by Projekt DEAL.

Data availability Market research data for Fig. 3 available on request.

Compliance with ethical guidelines

Conflict of interest The authors declare that they have no conflict of interest.

Code availability Not applicable for that section.

Nomenclature A, Surface; a_e, *Width of cut*; A_{fluid}, Flow velocity of fluid; a_p, *Depth of cut*; c, Specific heat capacity; CFRP, Carbon fiber reinforced plastic; d_T, End mill diameter; $d\theta_{in/out}$, Temperature difference between inner and outer bearing ring; e, Bearing clearance; e_{ax}, Bearing axial clearance; e_{rad}, Bearing radial clearance; E_M, Machining error; F_{ce}, Centrifugal force; F_{com}, Combined preload; F_{ext}, External force; F_{pre}, Bearing preload force; $F_{pre,in}$, Initial bearing preload force; f_z, Feed per tooth; $h_{l,ex}$, Average expected life hours; l, Length; l_m, Measuring distance; M_{gt}, Gyroscopic torque; n, Rotational speed; *NC*, Numerical Control; n_z, Number of teeth; P_M, Motor power; Q, Thermal energy; $\dot{Q}$, Heat flow; Ra, Arithmetic average roughness; Rz, Mean roughness depth; $r_{gr,\ i}$, Distance between bearing axle and bearing groove at inner ring; $r_{gr,\ o}$, Distance between bearing axle and bearing groove at outer ring; r_{re}, Radius of rolling element; $r_{rw.\ i}$, Inner groove radius; $r_{rw.\ o}$, Outer groove radius; TCP, Tool center point; $t_{stat,\ cool}$, Time to reach a colder steady state; $t_{stat,\ heat}$, Time to reach a warmer steady state; V, Volume; $\dot{V}$, Flow rate; v_C, Cutting speed; v_f, Feed velocity; v_{fluid}, Flow cross-section of fluid; α, Heat transfer coefficient; β, Contact angle; β_0, Assembly contact angle; $\beta_{op,\ i}$, Operation contact angle at bearing inner ring; $\beta_{op,\ o}$, Operation contact angle at bearing outer ring; γ, Coefficient of thermal expansion; $\gamma_{m,\ i}$, Coefficient of thermal expansion of inner bearing ring material; $\gamma_{m,\ o}$, Coefficient of thermal expansion of outer bearing ring material; $\gamma_{m,\ re}$, Coefficient of thermal expansion of rolling element

material; θ, Temperature; θ_0, Initial temperature; $\theta_{b,\ i}$, Mean temperature bearing inner ring; $\theta_{b,\ o}$, Mean temperature bearing outer ring; θ_{cool}, Temperature during cooling phase; $\theta_{fluid,in}$, Temperature of inlet fluid; $\theta_{fluid,out}$, Temperature of outlet fluid; θ_{heat}, Temperature during warm-up phase; θ_{lim}, Temperature limit value; θ_{stat}, Temperature at steady state; θ_W, Winding temperature; κ, Bearing osculation; ρ, Density; χ_{loss}, Loss fraction; ω, Angular velocity

References

1. Taniguchi N (1983) Current status in, and future trends of, ultraprecision machining and ultrafine materials processing. CIRP Ann Manuf Technol 32(2):573–582. https://doi.org/10.1016/S0007-8506(07)60185-1
2. Brecher C, Shneor Y, Neus S, Bakarinow K, Fey M (2015) Thermal behavior of externally driven spindle: experimental study and modelling. Engineering 7(2):73–92. https://doi.org/10.4236/eng.2015.72007
3. Pan X, He X, Wei K, Wu H, Gao J, Jiang Z (2019) Performance Analysis and Experimental research of electromagnetic-ring active balancing actuator hollow rotors of machine tool spindles. Appl Sci 9(4):692. https://doi.org/10.3390/app9040692
4. Fan H, Wang J, Shao S, Jing M, Liu H, Zhang X (2020) A Corrected Adaptive Balancing Approach of motorized spindle considering air gap unbalance. Appl Sci 10(6):2197. https://doi.org/10.3390/app10062197
5. Gao S, Cheng K, Ding H, Fu H (2016) Multiphysics-based design and analysis of the high-speed aerostatic spindle with application to micro-milling. Proceedings of the Institution of Mechanical Engineers. Part J: J Eng Tri 230(7):852–871. https://doi.org/10.1177/1350650115619609
6. Castro HFF (2008) A method for evaluating spindle rotation errors of machine tools using a laser interferometer. Measurement 41(5):526–537. https://doi.org/10.1016/j.measurement.2007.06.002
7. Marsh E (2009) Precision spindle metrology, 2nd edn. DEStech Publications, Lancaster
8. Abele E, Altintas Y, Brecher C (2010) Machine tool spindle units. CIRP Ann Manuf Technol 59(2):781–802. https://doi.org/10.1016/j.cirp.2010.05.002
9. Götz T (2006) Hydraulisch übersetzter Piezostapelaktor zur Vorspannungsregelung einer wälzgelagerten Werkzeugspindel. Leibniz University Hannover, Dissertation
10. Gebert K (1997) Ein Beitrag zur thermischen Modellbildung von schnelldrehenden Motorspindeln. Dissertation, RWTH Aachen
11. Brecher C, Wissmann A (2011) Compensation of thermo-dependent machine tool deformations due to spindle load: investigation of the optimal transfer function in consideration of rough machining. Prod Eng 5(5):565–574. https://doi.org/10.1007/s11740-011-0311-4
12. Putz M, Richter C, Regel J, Bräunig M (2018b) Industrial consideration of thermal issues in machine tools. Prod Eng 12(6):723–736. https://doi.org/10.1007/s11740-018-0848-6
13. Milberg J (1992) Werkzeugmaschinen - Grundlagen. Zerspantechnik, Dynamik, Baugruppen und Steuerungen. Springer, Berlin
14. Weck M, Koch A (1993) Spindle bearing systems for high-speed applications in machine tools. Annals of the CIRP 42(1):445–448. https://doi.org/10.1016/S0007-8506(07)62482-2
15. Weck M (1990) Konstruktion von Spindel-Lager-Systemen für die Hochgeschwindigkeits-Materialbearbeitung. Fertigungstechnologische Forderungen, technischer Stand, konstruktive Gestaltung, zukünftige Entwicklung. Expert, Ehningen
16. Jorgensen BR, Shin YC (1997) Dynamics of machine tool spindle/bearing systems under thermal growth. J Tribol 119(4):875–882. https://doi.org/10.1115/1.2833899
17. Brecher C, Spachtholz G, Paepenmüller F (2007) Developments for high performance machine tool spindles. CIRP Ann Manuf Technol 56(1):395–399. https://doi.org/10.1016/j.cirp.2007.05.092
18. Weck M, Spachtholz G (2003) 3- and 4-contact point spindle bearings - a new approach for high speed spindle systems. Annals of the CIRP 52(1):311–316. https://doi.org/10.1016/S0007-8506(07)60591-5
19. Kakino Y (2004) Latest trend of main spindle for NC machine tool. NTN Tech Rev 72:2–5
20. Moriwaki T (2006) Trends in recent machine tool technologies. NTN Tech Rev 74:2–7
21. Nakamura S (2012) Technology development and future challenge of machine tool spindle. J SME-Japan 1(1):1–7
22. Tako H, Tanaka Y (2010) Technical trend of machine tool bearings. NTN Tech Rev 78:10–14
23. de Ciurana J, Quintana G, Campa FJ (2009) Machine tool spindles. In: Lamikiz A (ed) López de Lacalle LN. Machine tools for high performance machining, Springer, London, pp 75–127. https://doi.org/10.1007/978-1-84800-380-4
24. Mori M, Fujishima M, Kashihara K, Horikawa M (2005) Development and application of a direct drive motor for performance enhancement of versatile machine tool systems. CIRP Ann Manuf Technol 54(1):337–340. https://doi.org/10.1016/S0007-8506(07)60117-6
25. Todkar SS, Chhapkhane NK, Todkar SR (2012) Recent advances in machine tool spindle technology. In: International Conference on Materials Processing and Characterization. Hyderabad, 8-10 March 2012. pp 196-202. https://www.researchgate.net/publication/323551949_Recent_advances_in_machine_tool_spindle_technology.
26. Boglietti A, Cavagnino A, Tenconi A, Vaschetto S (2009) Key design aspects of electrical machines for high-speed spindle applications. In: 36th Annual Conference on IEEE Industrial Electronics Society. Glendale, 7-10 Nov. 2010. pp 1735-1740, https://doi.org/10.1109/IECON.2010.5675417
27. Denkena B, Bergmann B, Klemme H, Dahlmann D (2018) Cooling potential of heat pipes and heat exchangers within a machine tool spindle. In: Ihlenfeldt S, Brecher C, Putz M, Billington D (eds) Conference on Thermal Issues in Machine Tools: Proceedings 2018, 1st edn. Wissenschaftliche Scripten, Auerbach/Vogtland, pp 295–305
28. Spur G (1996) Die Genauigkeit von Maschinen - Eine Konstruktionslehre. Carl Hanser, Munich
29. Putz M, Richter C, Regel J, Bräunig M (2018a) Industrial relevance and causes of thermal issues in machine tools. In: Ihlenfeldt S, Brecher C, Putz M, Billington D (eds) Proceedings Conference on Thermal Issues in Machine Tools, 1st edn. Wissenschaftliche Scripten, Auerbach/Vogtland, pp 127–139
30. Lamikiz A, López de Lacalle LN, Celaya A (2009) Machine tool performance and precision. In: López de Lacalle LN, Lamikiz A

(eds) Machine tools for high performance machining, Springer, London, pp 219-260. https://doi.org/10.1007/978-1-84800-380-4_6
31. López de Lacalle LN, Lamikiz A, Muñoa J, Salgado MA, Sánchez JA (2006) Improving the high-speed finishing of forming tools for advanced high-strength steels (AHSS). Int J Adv Manuf Technol 29(1-2):49–63. https://doi.org/10.1007/s00170-004-2482-z
32. Chatterjee S (1996) Spindle deflections in high-speed machine tools - modelling and simulation. Int J Adv Manuf Technol 11: 232–239. https://doi.org/10.1007/BF01351280
33. Slocum AH (1992) Precision machine design. SME, Dearborn
34. Gomez-Acedo E, Olarra A, Zubieta M, Kortaberria G, Arriznabarreta E, López de Lacalle LN (2015) Method for measuring thermal distortion in large machine tools by means of laser multilateration. Int J Adv Manuf Technol 80(1-4):523–534. https://doi.org/10.1007/s00170-015-7000-y
35. Mayr J, Jedrzejewski J, Uhlmann E, Alkan Donmez M, Knapp W, Härtig F, Wendt K, Moriwaki T, Shore P, Schmitt R, Brecher C, Würz T, Wegener K (2012) Thermal issues in machine tools. CIRP Ann 61(2):771–791. https://doi.org/10.1016/j.cirp.2012.05.008
36. Grama SN, Mathur A, Aralaguppi R, Subramanian T (2017) Optimization of high speed machine tool spindle to minimize thermal distortion. Procedia CIRP 58:457–462. https://doi.org/10.1016/j.procir.2017.03.253
37. Uhlmann E, Hu J (2012) Thermal modelling of a high speed motor spindle. Procedia CIRP 1:313–318. https://doi.org/10.1016/j.procir.2012.04.056
38. Liu Z, Pan M, Zhang A, Zhao Y, Yang Y, Ma C (2015) Thermal characteristic analysis of high-speed motorized spindle system based on thermal contact resistance and thermal-conduction resistance. Int J Adv Manuf Technol 76(9-12):1913–1926. https://doi.org/10.1007/s00170-014-6350-1
39. Creighton E, Honegger A, Tulsian A, Mukhopadhyay D (2010) Analysis of thermal errors in a high-speed micro-milling spindle. Int J Mach Tools Manuf 50(4):386–393. https://doi.org/10.1016/j.ijmachtools.2009.11.002
40. Haitao Z, Jianguo Y, Jinhua S (2007) Simulation of thermal behavior of a CNC machine tool spindle. Int J Mach Tools Manuf 47(6):1003–1010. https://doi.org/10.1016/j.ijmachtools.2006.06.018
41. Lin C-J, Su X-Y, Hu C-H, Jian B-L, Wu L-W, Yau H-T (2020) A linear regression thermal displacement lathe spindle model. Energies 13(4):949. https://doi.org/10.3390/en13040949
42. Liang F, Gao J, Xu L (2020) Investigation on a grinding motorized spindle with miniature-revolving-heat-pipes central cooling structure. Int Commu Heat Mass Transfer 112:104502. https://doi.org/10.1016/j.icheatmasstransfer.2020.104502
43. H-t Y, Guo C-g, Li Q, L-j Z, G-b H (2020) Thermal error modeling of CNC milling machine tool spindle system in load machining: based on optimal specific cutting energy. J Braz Soc Mech Sci Eng 42(9):1235. https://doi.org/10.1007/s40430-020-02538-5
44. Ge Z, Ding X (2018) Design of thermal error control system for high-speed motorized spindle based on thermal contraction of CFRP. Int J Mach Tools Manuf 125:99–111. https://doi.org/10.1016/j.ijmachtools.2017.11.002
45. Spur G, Hoffmann E, Paluncic Z, Benzinger K, Nymoen H (1988) Thermal behaviour optimization of machine tools. CIRP Ann 37(1):401–405. https://doi.org/10.1016/S0007-8506(07)61664-3
46. Liu T, Gao W, Tian Y, Zhang D, Zhang Y, Chang W (2017) Power matching based dissipation strategy onto spindle heat generations. Appl Therm Eng 113:499–507. https://doi.org/10.1016/j.applthermaleng.2016.11.057
47. Li K-Y, Luo W-J, Hong X-H, Wei S-J, Tsai P-H (2020) Enhancement of machining accuracy utilizing varied cooling oil volume for machine tool spindle. IEEE Access 8:28988–29003. https://doi.org/10.1109/ACCESS.2020.2972580
48. Kim S-M, Lee S-K (2005) Spindle housing design parameter optimization considering thermo-elastic behaviour. Int J Adv Manuf Technol 25(11-12):1061–1070. https://doi.org/10.1007/s00170-003-1958-6
49. Mori M, Mizuguchi H, Fujishima M, Ido Y, Mingkai N, Konishi K (2009) Design optimization and development of CNC lathe headstock to minimize thermal deformation. CIRP Ann 58(1): 331–334. https://doi.org/10.1016/j.cirp.2009.03.033
50. Brecher C, Weck M (2017) Werkzeugmaschinen Fertigungssysteme, 9th edn. Springer Vieweg, Berlin
51. Jędrzejewski J, Kowal Z, Kwaśny W, Modrzycki W (2005) High-speed precise machine tools spindle units improving. J Mater Process Technol 162-163:615–621. https://doi.org/10.1016/j.jmatprotec.2005.02.149
52. Kim K-D, Kim M-S, Chung S-C (2004) Real-time compensatory control of thermal errors for high-speed machine tools. Proceedings of the Institution of Mechanical Engineers. Part B: J Eng Manuf 218(8):913–924. https://doi.org/10.1243/0954405041486163
53. Abuaniza A, Fletcher S, Longstaff AP (2013) Thermal error modelling of a three axes vertical milling machine using Finite element analysis (FEA), In: Proceedings of Computing and Engineering Annual Researchers' Conference 2013. Huddersfield, 1-4 Dec. 2013, pp 87-92
54. Abdulshahed AM, Longstaff AP, Fletcher S, Myers A (2015) Thermal error modelling of machine tools based on ANFIS with fuzzy c-means clustering using a thermal imaging camera. Appl Math Model 39(7):1837–1852. https://doi.org/10.1016/j.apm.2014.10.016
55. Veldhuis SC, Elbestawi MA (1995) A strategy for the compensation of errors in five-axis machining. CIRP Ann 44(1):373–377. https://doi.org/10.1016/S0007-8506(07)62345-2
56. Vyroubal J (2012) Compensation of machine tool thermal deformation in spindle axis direction based on decomposition method. Precis Eng 36(1):121–127. https://doi.org/10.1016/j.precisioneng.2011.07.013
57. Babu R, Raja VP, Kanchana J, Krishna DV (2014) Identification, development and testing of thermal error compensation model for a headstock assembly of CNC turning centre. Int J Eng Technol 3(2):113. https://doi.org/10.14419/ijet.v3i2.2012
58. Srivastava AK, Veldhuis SC, Elbestawit MA (1995) Modelling geometric and thermal errors in a five-axis cnc machine tool. Int J Mach Tools Manuf 35(9):1321–1337. https://doi.org/10.1016/0890-6955(94)00048-O
59. Gomez-Acedo E, Olarra A, Orive J, López de la Calle LN (2013) Methodology for the design of a thermal distortion compensation for large machine tools based in state-space representation with Kalman filter. Int J Mach Tools Manuf 75:100–108. https://doi.org/10.1016/j.ijmachtools.2013.09.005
60. Liu K, Liu Y, M-j S, Wu Y-l, Zhu T-j (2017) Comprehensive thermal growth compensation method of spindle and servo axis error on a vertical drilling center. International Journal of Advanced Manufacturing Technology volume 88(9-12):2507–2516. https://doi.org/10.1007/s00170-016-8972-y
61. Bossmanns B, Tu JF (1999) A thermal model for high speed motorized spindles. Int J Mach Tools Manuf 39(9):1345–1366. https://doi.org/10.1016/S0890-6955(99)00005-X
62. Grama SN, Mathur A, Badhe AN (2018) A model-based cooling strategy for motorized spindle to reduce thermal errors. Int J Mach Tools Manuf 132:3–16. https://doi.org/10.1016/j.ijmachtools.2018.04.004
63. Holkup T, Cao H, Kolář P, Altintas Y, Zelený J (2010) Thermo-mechanical model of spindles. CIRP Ann 59(1):365–368. https://doi.org/10.1016/j.cirp.2010.03.021
64. Hsieh K-H, Chen T-R, Chang P, Tang C-H (2013) Thermal growth measurement and compensation for integrated spindles.

Int J Adv Manuf Technol 64(5-8):889–901. https://doi.org/10.1007/s00170-012-4041-3
65. Kim S-M, Lee S-K (2001) Prediction of thermo-elastic behavior in a spindle-bearing system considering bearing surroundings. Int J Mach Tools Manuf 41(6):809–831. https://doi.org/10.1016/S0890-6955(00)00103-6
66. Kolar P, Holkup T (2010) Prediction of machine tool spindle's dynamics based on a thermo-mechanical model. MM Science Journal 2010(1):167–171. https://doi.org/10.17973/MMSJ.2010_03_201002
67. Liu T, Gao W, Zhang D, Zhang Y, Chang W, Liang C, Tian Y (2017) Analytical modeling for thermal errors of motorized spindle unit. Int J Mach Tools Manuf 112:53–70. https://doi.org/10.1016/j.ijmachtools.2016.09.008
68. Liu J, Zhang P (2018) Thermo-mechanical behavior analysis of motorized spindle based on a coupled model. Adv Mech Eng 10(1):168781401774714. https://doi.org/10.1177/1687814017747144
69. Kim J-D, Zverv I, Lee K-B (2010) Thermal model of high-speed spindle units. Intell Inf Manag 2(5):306–315. https://doi.org/10.4236/iim.2010.25036
70. Zhang X, Yu S, Lou P, Jiang X, Hu J, Yan J (2019) Thermal error exponential model of CNC machine tools motorized spindle based on mechanism analysis. In: 11th International Conference on Intelligent Human-Machine Systems and Cybernetics. Hangzhou, 24-25 Aug. 2019, pp 291-295. https://doi.org/10.1109/IHMSC.2019.00074
71. Shi X, Yang X, Mu Y, Wang Y, Wang W (2019) Thermal error compensation model for a motorized spindle with shaft core cooling based on exponential function. Int J Adv Manuf Technol 103(9-12):4805–4813. https://doi.org/10.1007/s00170-019-04038-w
72. Brecher C, Ihlenfeldt S, Neus S, Steinert A, Galant A (2019) Thermal condition monitoring of a motorized milling spindle. Prod Eng 13(5):539–546. https://doi.org/10.1007/s11740-019-00905-3
73. Li Y, Zhao W, Lan S, Ni J, Wu W, Lu B (2015) A review on spindle thermal error compensation in machine tools. Int J Mach Tools Manuf 95:20–38. https://doi.org/10.1016/j.ijmachtools.2015.04.008
74. Fujii K, Shimuzu S, Mori M (2001) Preload control technology of rolling bearings for machine tool spindles. Journal of the Japan Society for Precision Engineering 67(3):418–422. https://doi.org/10.2493/jjspe.67.418
75. Kim K, Kim SS (1989) Effect of preload on running accuracy of spindle. Int J Mach Tools Manuf 29(1):99–105. https://doi.org/10.1016/0890-6955(89)90058-8
76. Bossmanns B, Tu JF (2001) A power flow model for high speed motorized spindles - heat generation characterization. J Manuf Sci Eng 123(3):494–505. https://doi.org/10.1115/1.1349555
77. Tüllmann U (1999) Das Verhalten axial verspannter schnelldrehender Schrägkugellager. Dissertation, RWTH Aachen
78. Boglietti A, Ferraris P, Lazzari M, Profumo F (1992) About the design of very high frequency induction motors for spindle applications. In: Conference record of the 1992 IEEE Industry Applications Society Annual Meeting. Houston, 4-9 Oct. 1992, pp 25-32. https://doi.org/10.1109/IAS.1992.244469
79. Nakamura S, Kakino Y (1992) An analysis on preload increment and displacement of a rotating high speed spindle. Journal of the Japan Society for Precision Engineering 58(12):2019–2024. https://doi.org/10.2493/jjspe.58.2019
80. Walter R (2006) Mit direkter Kühlung zu mehr Genauigkeit. WB - Werkstatt und Betrieb 139(6):129–130
81. Butz F (2007) Gestaltung der Loslagerung von Werkzeugmaschinenspindeln. Dissertation, RTWH Aachen
82. GMN Paul Müller Industrie GmbH & Co. KG (2019) Lagerschmierung. https://www.gmn.de/kugellager/engineering/schmierung/.
83. Berg F (1990) Elektromotoren mit hohem Wirkungsgrad: Auslegung, wirtschaftliche Aspekte und Entwicklungstendenzen. Schweizer Ingenieur und Architekt 108(38):1059–1061
84. Lu T (2004) Weiterentwicklung von hochtourigen permanenterregten Drehstromantrieben mit Hilfe von Finite-Elemente-Berechnungen und experimentellen Untersuchungen. Dissertation, TU Darmstadt
85. Yang Y, Bilgin B, Kasprzak M, Nalakath S, Sadek H, Preindl M, Cotton J, Schofield N, Emadi A (2017) Thermal management of electric machines. IET Electrical Systems in Transportation 7(2):104–116. https://doi.org/10.1049/iet-est.2015.0050
86. Sebastian T (1995) Temperature effects on torque production and efficiency of PM motors using NdFeB magnets. IEEE Trans Ind Appl 31(2):353–357. https://doi.org/10.1109/28.370284
87. Yoon MK, Jeon CS, Kauh SK (2002) Efficiency increase of an induction motor by improving cooling performance. IEEE Transactions on Energy Conversion 17(1):1–6. https://doi.org/10.1109/60.986430
88. Funieru B, Binder A (2008) Thermal design of a permanent magnet motor used for gearless railway traction. In: 34th Annual Conference of IEEE Industrial Electronics. Orlando, 10-13 Nov. 2008. IEEE, pp 2061-2066. https://doi.org/10.1109/IECON.2008.4758274
89. Galea M, Gerada C, Raminosoa T, Wheeler P (2012) A Thermal improvement technique for the phase windings of electrical machines. IEEE Trans Ind Appl 48(1):79–87. https://doi.org/10.1109/TIA.2011.2175470
90. Tanner R (1997) The selection of energy-efficient motors from catalogues. In: Almeida A, Bertoldi P, Leonhard W (eds) Energy Efficiency Improvements in Electric Motors and Drives, 1st edn. Springer, Berlin/Heidelberg, pp 503–511. https://doi.org/10.1007/978-3-642-60832-2_40
91. IEEE (2016) IEEE standard test procedures for evaluation of systems of insulating materials for random-wound ac electric machinery. Revision of ANSI C50.32-1976 and IEEE Std 117-1974 (Revision of IEEE Std 177-1974). https://doi.org/10.1109/IEEESTD.2016.7466454
92. Lehrmann C, Yogal N (2016) PM-Synchronmaschine - hohe Energieeffizienz auch in Ex-Bereichen? Antriebstechnik 55(3):80–83
93. Li H, Ying X, Heisel U (2009) Optimization design for CNC machine spindle system heat-dissipating structure. In: International Conference on Mechatronics and Automation. Changchun, 9-12 Aug. 2009. IEEE, pp 1406-1410. https://doi.org/10.1109/ICMA.2009.5246674
94. Grabowski M, Urbaniec K, Wernik J, Wołosz KJ (2016) Numerical simulation and experimental verification of heat transfer from a finned housing of an electric motor. Energy Convers Manag 125:91–96. https://doi.org/10.1016/j.enconman.2016.05.038
95. Ponnappan R, Leland JE (1998) Rotating heat pipe for high speed motor/generator cooling. SAE Trans 107:167–172. https://doi.org/10.4271/981287
96. Kruckow W, Pfeiffer R, Werth L (1989) Einfluss der Luftspaltweite auf die Verluste schnellaufender Asynchronmaschine mit Käfigläufer. Archiv für Elektrotechnik 72:427–434
97. Lehrmann C, Lienesch F, Engel U, (2002) Oberschwingungsverluste und Erwärmungen umrichtergespeister Induktionsmaschinen. Bestimmung der Verluste in Abhängigkeit der Betriebsparameter. Bulletin SEV/VSE (15):9-14
98. Rothenbücher S, Schiffler A, Bauer J (2009) Die Speisung macht's. Temperaturverhalten schnell drehender Spindeln. WB Werkstatt + Betrieb (7-8):62-65

99. Weiss L, Züst S (2014) Vorrichtung zur Kühlung von Maschinenbauteilen mittels PCM. Patent no. EP 2 949 422 B1
100. Bradford M (1989) The application of heat pipes to cooling rotating electrical machines. 4th International Conference on Electrical Machines and Drives. London, 13-15 Sep. 1989. IET, pp 145-149
101. Potoradi D, Vollmer R (2003) Electric machine with heat pipes. Patent no. US 6,943,467 B2
102. Hassett T, Hodowanec M (2007) Electric motor with heat pipes. Patent no. US 7,569,955 B2
103. Kaiser M, Soghomonian ZS (2004) Dynamolectric machine having heat pipes embedded in stator core. Patent no. US 7,635,932 B2
104. Putra N, Ariantara B (2017) Electric motor thermal management system using L-shaped flat heat pipes. Appl Therm Eng 126:1156–1163. https://doi.org/10.1016/j.applthermaleng.2017.01.090
105. Groll M, Krahling H, Munzel WD (1978) Heat pipes for cooling of an electric motor. Journal of Energy 2(6):363–367. https://doi.org/10.2514/3.62387
106. Corman, JC, Edgar RF, McLaughlin MH, Tompkins RE (1972) Rotating electrical machine having rotor and stator cooled by means of heat pipes. Patent no. US 3,801,843 A
107. Huang J, Shoai Naini S, Miller R, Rizzo D, Sebeck K, Shurin S, Wagner J (2019) A hybrid electric vehicle motor cooling system - design, model, and control. IEEE Trans Veh Technol 68(5):4467–4478. https://doi.org/10.1109/TVT.2019.2902135
108. Uhlmann E, Polte J, Salein S, Iden N, Temme R, Hartung D, Perschewski S (2020) Entwicklung einer thermo elektrisch temperierten Motorspindel: Reduktion thermisch bedingter Verlagerungen durch Integration von Peltierelementen in eine Hochfrequenzmotorspindel. wt. WerkstattsTechnik 110(5):299–305
109. Koreta N, Jinno K, Rokkaku T, Mizuta K, Watanabe K (1994) Thermoelectric Cooling of Machine Tool Spindle. Journal of the Japan Society for Precision Engineering 60(5):652–656. https://doi.org/10.2493/jjspe.60.652
110. Wegener K, Mayr J, Merklein M, Behrens B-A, Aoyama T, Sulitka M, Fleischer J, Groche P, Kaftanoglu B, Jochum N, Möhring HC (2017) Fluid elements in machine tools. CIRP Ann Manuf Technol 66(2):611–634. https://doi.org/10.1016/j.cirp.2017.05.008
111. Kral C, Haumer A, Bauml T (2008) Thermal model and behavior of a totally-enclosed-water-cooled squirrel-cage induction machine for traction applications. IEEE Trans Ind Electron 55(10):3555–3565. https://doi.org/10.1109/TIE.2008.927242
112. Link HF (1995) Cooling system for a motor spindle for a machine tool. Patent no. US 5,664,916 A
113. Qiang H, Yuan S, Fengzhang R, Lili L, Volinsky AA (2016) Numerical simulation and experimental study of the air-cooled motorized spindle. Proceedings Institution of Mechanical Engineers. Part C: J Mechan Eng Sci 231(12):2357–2369. https://doi.org/10.1177/0954406216631781
114. Donmez MA, Hahn MH, Soons JA (2007) A novel cooling system to reduce thermally-induced errors of machine tools. CIRP Ann Manuf Technol 56(1):521–524. https://doi.org/10.1016/j.cirp.2007.05.124
115. Koepfer C (2001) Thermally stabilize spindles with air. https://www.mmsonline.com/articles/thermally-stabilize-spindles-with-air.
116. Czudaj M (2015) CNC-Mehrspindeldrehautomat INDEX MS52C3. https://de.industryarena.com/files/news/pressreleases/5794/INDEX_MS52C_DE.pdf.
117. Tüysüz A, Meyer F, Steichen M, Zwyssig C, Kolar JW (2017) Advanced cooling methods for high-speed electrical machines. IEEE Trans Ind Appl 53(3):2077–2087. https://doi.org/10.1109/TIA.2017.2672921
118. Tüysüz A, Steichen M, Zwyssig C, Kolar JW (2015) Advanced cooling concepts for ultra-high-speed machines. In: 9th International Conference on Power Electronics and ECCE Asia. Seoul, 1-5 June 2015, pp 2194-2202. https://doi.org/10.1109/ICPE.2015.7168081
119. Stöhr G (2007) Untersuchungen zum Aufbau einer hocheffizienten Kühlung einer elektrischen Maschine mit großer Leistungsdichte. Dissertation, TU Berlin
120. Chang C-F, Chen J-J (2009) Thermal growth control techniques for motorized spindles. Mechatronics 19(8):1313–1320. https://doi.org/10.1016/j.mechatronics.2009.06.012
121. Weber J, Shabi L, Weber J (2017) State of the art and optimization of the energy flow in cooling systems of motorized high-speed spindles in machine tools. Procedia CIRP 67:81–86. https://doi.org/10.1016/j.procir.2017.12.180
122. Chien CH, Jang JY (2008) 3-D numerical and experimental analysis of a built-in motorized high-speed spindle with helical water cooling channel. Appl Therm Eng 28(17-18):2327–2336. https://doi.org/10.1016/j.applthermaleng.2008.01.015
123. Huang J-H, Than V-T, Ngo T-T, Wang C-C (2016) An inverse method for estimating heat sources in a high speed spindle. Appl Therm Eng 105:65–76. https://doi.org/10.1016/j.applthermaleng.2016.05.123
124. Javelov IS (1983) Projektierung von Kühlsystemen für Elektrospindeln. Stanki i Instrument 54(4):25–26
125. Link HF, Grossmann W (1994) Motorspindel für eine Werkzeugmaschine Patent no WO 1994023485:A1
126. Sathiya Moorthy R, Prabhu Raja V, Lakshmipathi R (2012) Analysis of high speed spindle with a double helical cooling channel. Int J Sci Eng Res 3(5):1112–1116
127. Weber J, Weber J (2013) Thermo-energetic analysis and simulation of the fluidic cooling system of motorized high-speed spindles. In: Proceedings 13th Scandinavian International Conference on Fluid Power. Linköping 3-5 June, pp 131-140. https://doi.org/10.3384/ecp1392a14
128. Weber J, Shabi L, Weber J (2016) Thermal impact of different cooling sleeve's flow geometries in motorized high-speed spindles of machine tools. In: Proceedings of 9th FPNI PhD Symposium on Fluid Power. Florianópolis, 26-28 Oct. 2016. 10.1115/FPNI2016-1517
129. Xia C, Fu J, Lai J, Yao X, Chen Z (2015) Conjugate heat transfer in fractal tree-like channels network heat sink for high-speed motorized spindle cooling. Applied Thermal Engineering 901032-1042. https://doi.org/10.1016/j.applthermaleng.2015.07.024
130. Li K-Y, Luo W-J, Wei S-J (2020) Machining accuracy enhancement of a machine tool by a cooling channel design for a built-in spindle. Appl Sci 10(11):3991. https://doi.org/10.3390/app10113991
131. Huang Y-H, Huang C-W, Chou Y-D, Ho C-C, Lee M-T (2016) An experimental and numerical study of the thermal issues of a high-speed built-in motor spindle. Smart Science 4(3):160–166. https://doi.org/10.1080/23080477.2016.1214062
132. Mansingh BB, Pravin APA (2010) Simulation of axial cooling loop for high speed spindles with rectangular crossection using CFD. In: Conference: Frontiers in Automobile and Mechanical Engineering. Chennai, 25-27 Nov. 2010. IEEE, pp 265-268. https://doi.org/10.1109/FAME.2010.5714832
133. Li K-Y, Luo W-J, Wei S-J, Liao Y-s (2020) Cooling channel design for a built-in spindle of a machine tool. J Phys Conf Ser 1500:012031. https://doi.org/10.1088/1742-6596/1500/1/012031
134. Chen N, Zhang K, Zhang LX, Wu YH (2014) Analysis on the effects of cooling water velocity on temperature rise of motorized spindle. Appl Mech Mater 543–547:68–71. https://doi.org/10.4028/www.scientific.net/amm.543-547.68

135. Wu C-H, Kung Y-T (2004) A parametric study on oil/air lubrication of a high-speed spindle. Precis Eng 29(2):162–167. https://doi.org/10.1016/j.precisioneng.2004.06.005
136. Li S, Wu, Y (2010) A study on oil/air lubrication and preload of a high frequency fully ceramic motor spindle. In: International Conference on E-Product E-Service and E-Entertainment. Henan, 7-9 Nov. 2010. IEEE, pp 3611-3614. https://doi.org/10.1109/ICEEE.2010.5661555
137. Zhang L, Yu S, Wu Y, Zhang K, Shi Q, An D (2019) Parameter optimization of a motorized spindle lubrication system using biogeography-based optimization. Adv Mech Eng 11(1): 168781401881988. https://doi.org/10.1177/1687814018819889
138. Onda Y, Fukada K, Yamamoto Y, Yoshino M (2014) Machine tool main spindle bearings with air cooling spacer. NTN Tech Rev 82:38–43
139. Onda Y, Mizutani M, Mori M (2002) Machine tool main spindle bearings with "air cooling spacer". NTN Tech Rev 80:38–41
140. Baldwin, HJ (1964) Machine tool spindle cooling system. Patent no. US 3,221,606 A
141. Ma H, Du D, Sun J, Zhang Y, Deng N (2011) Convective mass transfer from a horizontal rotating cylinder in a slot air jet flow. Int J Heat Mass Transf 54(1-3):186–193. https://doi.org/10.1016/j.ijheatmasstransfer.2010.09.054
142. Dong, QJ, Chen C-L (2004) Motor rotor cooling with rotation heat pipes. Patent no. US 7,443,062 B2
143. Fedoseyev L, Pearce EM (2013) Rotor assembly with heat pipe cooling system. Applied for by Tesla Motors, Inc. on 7/13/2013. Patent no. US 2014/0368064 A1
144. Harano K, Oyama S (1978) Rotary electric machine with a heat pipe for cooling. Patent no. US 4,240,000 A
145. Harano K, Kawada S, Oyama S (1981) Rotary electric motor Patent no EP 0039493:B1
146. Khanh D (1993) Electric motor having internal heat dissipator. Applied for by Heat Pipe Technology Inc. Patent no. US 5,394,040 A
147. König H, Canders W-R, Brost O, Braun H, Unk J (1988) Drehende Maschine mit Wärmerohr-Kühlung Patent no EP 0152785:B1
148. Dong, QJ, Chen C-L (2004) Motor rotor cooling with rotation heat pipes. Patent no. US 2006/0066156 A1
149. Workman J (1976) Cooling system for electric motors. Patent no. US 4,137,472 A
150. Polasek F (1973) Cooling of a.c. motor by heat pipes. In: Groll M, Keser D (eds): Proceedings 1st International Heat Pipe Conference. Stuttgart, 15 Oct. 1973
151. Marto PJ (1982) Rotating heat pipes. In: Proceedings 14th Symposium of the International Centre for Heat and Mass Transfer (ICHMT). Dubrovnik, 29 Aug.- 02 Sep.
152. Ponnappan R, Beam JE, Leland JE (1995) Electric machine. Patent no. US 5,629,573 A
153. Heintz RM (1940) Motor cooling system. Patent no. US 2,330,121 A
154. Faistauer F, Gumpoldsberger T (2014) Elektrische Maschine Patent no DE 102014202056:A1
155. Yerkes KL (1990) Technology review: Utilizing rotating thermosiphon technology in aircraft thermal management and control. J Aerospace 99:1996–2066
156. Judd RL, Aftab K, Elbestawi MA (1994) An investigation of the use of heat pipes for machine tool spindle bearing cooling. Int J Mach Tools Manuf 34(7):1031–1043. https://doi.org/10.1016/0890-6955(94)90033-7
157. Hashimoto R, Mizuta K, Itani H, Kura K, Takahashi Y (1996) Heat transport performance of rotating heat pipes installed in high-speed spindle. Mitsubishi Heavy Industries, Ltd. Technical Review 33(2):88–92
158. Liang F, Gao J, Li F, Xu L, Wang Z, Jiang H (2019) A central cooling structure for motorized spindles: principle and application. In: Proceedings of 18th IEEE Intersociety Conference on Thermal and Thermomechanical Phenomena in Electronic Systems. Las Vegas, 28-31 May 2019. IEEE, pp 1204-1211. https://doi.org/10.1109/ITHERM.2019.8757403
159. Li F, Gao J, Shi X, Liang F, Zhu K (2018) Experimental investigation of single loop thermosyphons utilized in motorized spindle shaft cooling. Appl Therm Eng 134:229–237. https://doi.org/10.1016/j.applthermaleng.2017.11.141
160. Li F, Gao J, Shi X, Wang Z, Wang D (2020) Experimental investigation into rotating loop thermosyphons for cooling shafts of motorized spindles. Heat Mass Transf. https://doi.org/10.1007/s00231-020-02919-5
161. Yamada K (1985) Spindle bearing cooling structure (transl.). Patent no. 62-78245
162. Jankowski T (2007) Numerical and experimental investigations of a rotating heat pipe. PhD Thesis, University of New Mexico
163. Hoshi T, Shiraishi H (1998) Machine tool spindle. Patent no. JP 3616499 B2
164. Morimura S (2010) Cooling apparatus of main shaft. Patent no. JP 2012024878 A
165. Morimura S (2015) Development of new spindle cooling technology that concentrates cooling near front bearing. Int J Autom Technol 9(6):698–706. https://doi.org/10.20965/ijat.2015.p0698
166. Morimura S (2011) Cooling structure for machine tool main spindle. Patent no. US 08944731 B2
167. Morimura S, Shimomura R, Koto H, Yoshimura T (2013) Development of a low-cost spindle unit with a highly efficient spindle shaft cooling system ensuring high accuracy and high rigidity. Journal of the Japan Society for Precision Engineering 79(2):124–127. https://doi.org/10.2493/jjspe.79.124
168. P + L GmbH & Co. KG (2009) Werkzeugmaschine mit luftgekühlter Spindelwelle. DE 20 2009 009424 U1
169. Breitenberger A (2017) Das kalte Herz schlägt schneller. WB Werkstatt + Betrieb (10):51-53
170. Schneider K, Steffen D (2007) Wellenkühlung für eine Werkzeug-Motorspindel. Patent no. EP 2058085 B1
171. Scholl S (2006) Spindelvorrichtung mit Innenkühlung und geschlossenem Spindelkühlkanal durch eine Drehdurchführung. Patent no. EP 1736277 B1
172. Hiramoto K (1991) Apparatus for cooling a spindle bearing of a machine Patent no EP 0458499:B1
173. Walter R (2010) Kühlung für das Herzstück. Leistungsfähigere Spindeln durch Wellenkühlung. Schweizer Präzisions-Fertigungstechnik (1):40-42
174. Denkena B, Garber T (2013) NC Plus - Prozess- und wertschöpfungsorientiert gesteuerte Werkzeugmaschine: Abschlussbericht. PZH-Verlag, Garbsen
175. Abele E, Korff D (2011) Avoidance of collision-caused spindle damages - challenges, methods and solutions for high dynamic machine tools. CIRP Ann Manuf Technol 60(1):425–428. https://doi.org/10.1016/j.cirp.2011.03.031